Density Model for Killer Whale (*Orcinus orca*) for the U.S. East Coast: Supplementary Report

Model Version 2.1

Duke University Marine Geospatial Ecology Laboratory*

2023-05-27

Citation

When citing our methodology or results generally, please cite Roberts et al. (2016, 2023). The complete references appear at the end of this document. We are preparing a new article for a peer-reviewed journal that will eventually replace those. Until that is published, those are the best general citations.

When citing this model specifically, please use this reference:

Roberts JJ, Yack TM, Cañadas A, Fujioka E, Halpin PN, Barco SG, Boisseau O, Chavez-Rosales S, Cole TVN, Cotter MP, Cummings EW, Davis GE, DiGiovanni Jr. RA, Garrison LP, Gowan TA, Jackson KA, Kenney RD, Khan CB, Lockhart GG, Lomac-MacNair KS, McAlarney RJ, McLellan WA, Mullin KD, Nowacek DP, O'Brien O, Pabst DA, Palka DL, Quintana-Rizzo E, Redfern JV, Rickard ME, White M, Whitt AD, Zoidis AM (2022) Density Model for Killer Whale (*Orcinus orca*) for the U.S. East Coast, Version 2.1, 2023-05-27, and Supplementary Report. Marine Geospatial Ecology Laboratory, Duke University, Durham, North Carolina.

Copyright and License

Model Version History

Version	Date	Description
1	2015-01-31	Initial version.
1.1	2015-05-14	Updated calculation of CVs. Switched density rasters to logarithmic breaks. No changes to the model.
1.2	2015-09-26	Updated the documentation. No changes to the model. Model files released as supplementary information to Roberts et al. (2016).

---

*For questions or to offer feedback please contact Jason Roberts (jason.roberts@duke.edu) and Tina Yack (tina.yack@duke.edu)

(continued)

Version	Date	Description
2	2022-06-20	This model is a major update over the prior version, with substantial additional data, improved statistical methods, and an increased spatial resolution. It was released as part of the final delivery of the U.S. Navy Marine Species Density Database (NMSDD) for the Atlantic Fleet Testing and Training (AFTT) Phase IV Environmental Impact Statement. Several new collaborators joined and contributed survey data: New York State Department of Environmental Conservation, TetraTech, HDR, and Marine Conservation Research. We incorporated additional surveys from all continuing and new collaborators through the end of 2020. (Because some environmental covariates were only available through 2019, certain models only extend through 2019.) We increased the spatial resolution to 5 km and, at NOAA's request, we extended the model further inshore from New York through Maine. We reformulated and refitted all detection functions and spatial models. We updated all enviromental covariates to newer products, when available, and added several covariates to the set of candidates. For models that incorporated dynamic covariates, we estimated model uncertainty using a new method that accounts for both model parameter error and temporal variability.
2.1	2023-05-27	Completed the supplementary report documenting the details of this model. Corrected the 5 and 95 percent rasters so that they contain the value 0 where the taxon was asssumed absent, rather than NoData. Nothing else was changed.

1 Survey Data

We built this model from data collected between 1998-2020 (Table 1, Figure 1). We excluded surveys that only targeted large whales or were otherwise problematic for modeling smaller species. To maintain consistency with the other models developed during the 2022 modeling cycle, most of which excluded data prior to 1998 in order to utilize biological covariates derived from satellite ocean color observations, we also excluded data prior to 1998 from this model. We restricted the model to aerial survey transects with sea states of Beaufort 4 or less (for a few surveys we used Beaufort 3 or less) and shipboard transects with Beaufort 5 or less (for a few we used Beaufort 4 or less). We also excluded transects with poor weather or visibility for surveys that reported those conditions.

Table 1: Survey effort and observations considered for this model. Effort is tallied as the cumulative length of on-effort transects. Observations are the number of groups and individuals encountered while on effort. Off effort observations and those lacking an estimate of group size or distance to the group were excluded.

Institution	Program	Period	Effort 1000s km	Groups	Individuals	Mean Group Size
Aerial Surveys						
HDR	Navy Norfolk Canyon	2018-2019	11	0	0	
NEAq	CNM	2017-2020	2	0	0	
NEAq	MMS-WEA	2017-2020	37	0	0	
NEAq	NLPSC	2011-2015	43	0	0	
NEFSC	AMAPPS	2010-2019	83	1	3	3.0
NEFSC	NARWSS	2003-2016	380	3	8	2.7
NEFSC	Pre-AMAPPS	1999-2008	45	0	0	
NJDEP	NJEBS	2008-2009	9	0	0	
SEFSC	AMAPPS	2010-2020	112	0	0	
SEFSC	MATS	2002-2005	27	0	0	
UNCW	Navy Cape Hatteras	2011-2017	34	0	0	
UNCW	Navy Jacksonville	2009-2017	92	0	0	
UNCW	Navy Norfolk Canyon	2015-2017	14	0	0	
UNCW	Navy Onslow Bay	2007-2011	49	0	0	
VAMSC	MD DNR WEA	2013-2015	15	0	0	
VAMSC	Navy VACAPES	2016-2017	19	0	0	
VAMSC	VA CZM WEA	2012-2015	21	0	0	
	Total		**994**	**4**	**11**	**2.8**
Shipboard Surveys						
MCR	SOTW Visual	2012-2019	8	0	0	
NEFSC	AMAPPS	2011-2016	15	2	8	4.0
NEFSC	Pre-AMAPPS	1998-2007	11	0	0	
SEFSC	AMAPPS	2011-2016	16	1	5	5.0
SEFSC	Pre-AMAPPS	1998-2006	30	0	0	
	Total		**80**	**3**	**13**	**4.3**
	Grand Total		**1,075**	**7**	**24**	**3.4**

Table 2: Institutions that contributed surveys used in this model.

Institution	Full Name
HDR	HDR, Inc.
MCR	Marine Conservation Research
NEAq	New England Aquarium
NEFSC	NOAA Northeast Fisheries Science Center
NJDEP	New Jersey Department of Environmental Protection
SEFSC	NOAA Southeast Fisheries Science Center
UNCW	University of North Carolina Wilmington
VAMSC	Virginia Aquarium & Marine Science Center

Table 3: Descriptions and references for survey programs used in this model.

| Program	Description	References
AMAPPS	Atlantic Marine Assessment Program for Protected Species	Palka et al. (2017), Palka et al. (2021)
CNM	Northeast Canyons Marine National Monument Aerial Surveys	Redfern et al. (2021)
MATS	Mid-Atlantic Tursiops Surveys	
MD DNR WEA	Aerial Surveys of the Maryland Wind Energy Area	Barco et al. (2015)
MMS-WEA	Marine Mammal Surveys of the MA and RI Wind Energy Areas	Quintana-Rizzo et al. (2021), O'Brien et al. (2022)
NARWSS	North Atlantic Right Whale Sighting Surveys	Cole et al. (2007)
Navy Cape Hatteras	Aerial Surveys of the Navy's Cape Hatteras Study Area	McLellan et al. (2018)
Navy Jacksonville	Aerial Surveys of the Navy's Jacksonville Study Area	Foley et al. (2019)
Navy Norfolk Canyon	Aerial Surveys of the Navy's Norfolk Canyon Study Area	Cotter (2019), McAlarney et al. (2018)
Navy Onslow Bay	Aerial Surveys of the Navy's Onslow Bay Study Area	Read et al. (2014)
Navy VACAPES	Aerial Survey Baseline Monitoring in the Continental Shelf Region of the VACAPES OPAREA	Mallette et al. (2017)
NJEBS	New Jersey Ecological Baseline Study	Geo-Marine, Inc. (2010), Whitt et al. (2015)
NLPSC	Northeast Large Pelagic Survey Collaborative Aerial Surveys	Leiter et al. (2017), Stone et al. (2017)
Pre-AMAPPS	Pre-AMAPPS Marine Mammal Abundance Surveys	Mullin and Fulling (2003), Garrison et al. (2010), Palka (2006)
SOTW Visual	R/V Song of the Whale Visual Surveys	Ryan et al. (2013)
VA CZM WEA	Virginia CZM Wind Energy Area Surveys	Mallette et al. (2014), Mallette et al. (2015)
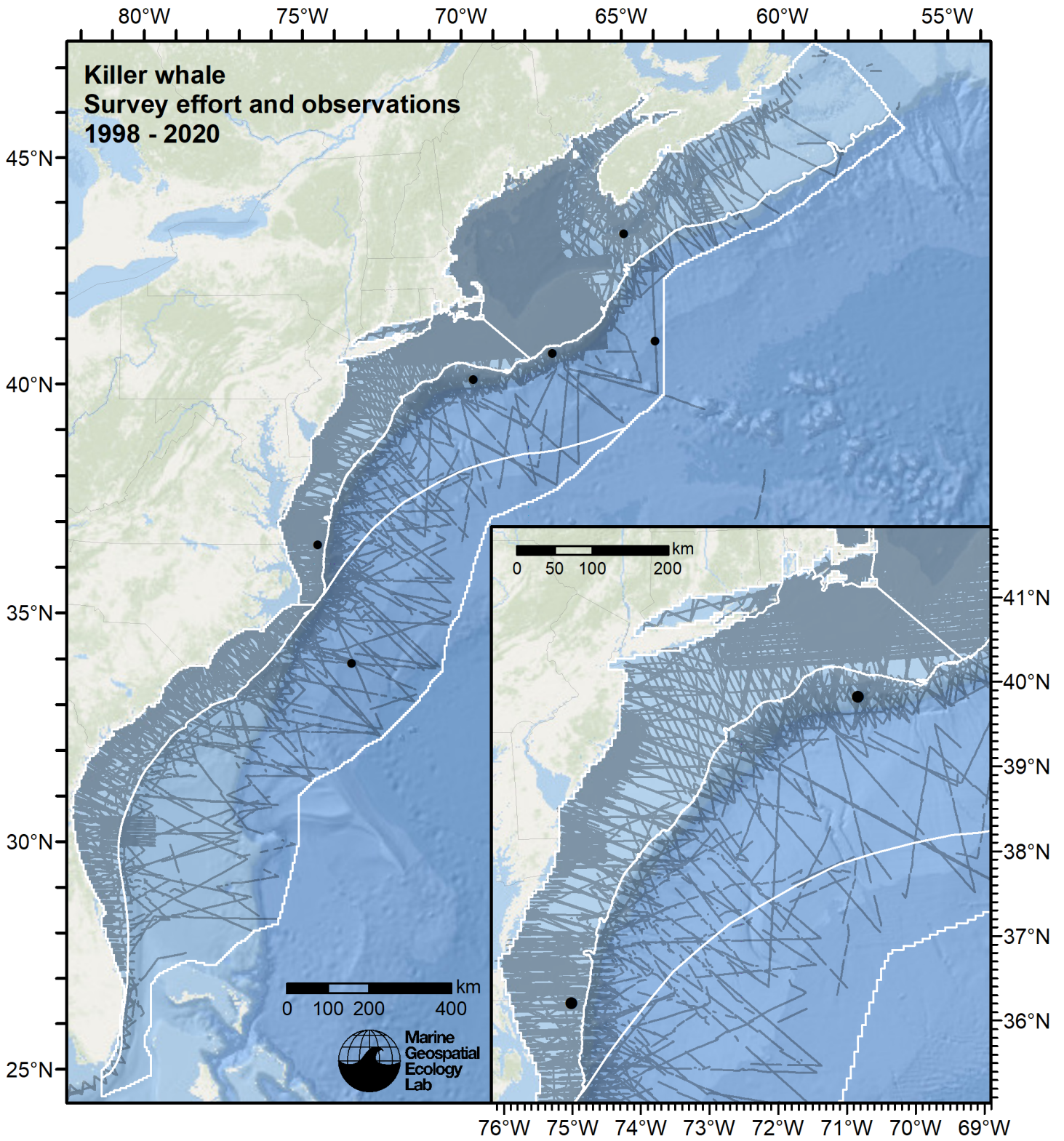
Figure 1: Survey effort and killer whale observations available for density modeling, after detection functions were applied, and excluded segments and truncated observations were removed. White outlines show the strata for which density estimates were derived.

2 Detection Functions

2.1 Without a Taxonomic Covariate

We fitted the detection functions in this section to pools of species with similar detectability characteristics but could not use a taxonomic identification as a covariate to account for differences between them. We usually took this approach after trying the taxonomic covariate and finding it had insufficient statistical power to be retained. We also resorted to it when the focal taxon being modeled had too few observations to be allocated its own taxonomic covariate level and was too poorly known for us to confidently determine which other taxa we could group it with.

2.1.1 Aerial Surveys

Figure 2: Detection hierarchy for aerial surveys, showing how they were pooled during detectability modeling, for detection functions that pooled multiple taxa but could not use a taxonomic covariate to account for differences between them. Each histogram represents a detection function and summarizes the perpendicular distances of observations that were pooled to fit it, prior to truncation. Observation counts, also prior to truncation, are shown in green when they met the recommendation of Buckland et al. (2001) that detection functions utilize at least 60 sightings, and red otherwise. For rare taxa, it was not always possible to meet this recommendation, yielding higher statistical uncertainty. During the spatial modeling stage of the analysis, effective strip widths were computed for each survey using the closest detection function above it in the hierarchy (i.e. moving from right to left in the figure). Surveys that do not have a detection function above them in this figure were either addressed by a detection function presented in a different section of this report, or were omitted from the analysis.

2.1.1.1 NEFSC Pre-AMAPPS

After right-truncating observations greater than 1300 m, we fitted the detection function to the 289 observations that remained (Table 4). The selected detection function (Figure 3) used a hazard rate key function with no covariates.

Table 4: Observations used to fit the NEFSC Pre-AMAPPS detection function.

ScientificName	n
Globicephala	148
Grampus griseus	141
Total	**289**
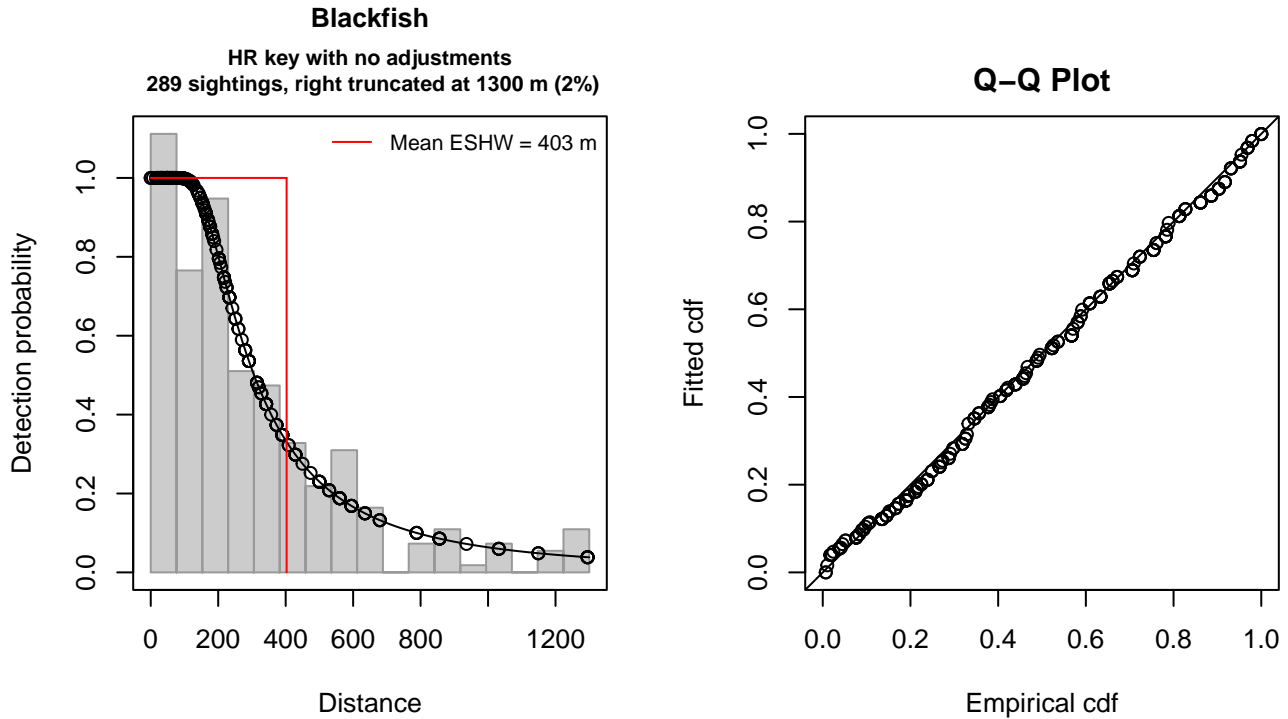
Figure 3: NEFSC Pre-AMAPPS detection function and Q-Q plot showing its goodness of fit.

Statistical output for this detection function:

```
Summary for ds object
Number of observations :  289
Distance range         :  0  -  1300
AIC                    :  3863.885

Detection function:
 Hazard-rate key function

Detection function parameters
Scale coefficient(s):
            estimate        se
(Intercept) 5.540493 0.1221542

Shape coefficient(s):
            estimate        se
(Intercept) 0.6890237 0.1060228
```

```
                    Estimate         SE          CV
Average p                  0.3098149   0.02386401 0.07702667
N in covered region 932.8151840 85.09243937 0.09122111


Distance sampling Cramer-von Mises test (unweighted)
Test statistic = 0.049395  p = 0.879943
```

2.1.1.2 NEFSC AMAPPS Protocol

After right-truncating observations greater than 400 m, we fitted the detection function to the 164 observations that remained (Table 5). The selected detection function (Figure 4) used a hazard rate key function with Beaufort (Figure 5) as a covariate.

Table 5: Observations used to fit the NEFSC AMAPPS Protocol detection function.

| ScientificName	n
Globicephala	76
Grampus griseus	87
Orcinus orca	1
Total	**164**
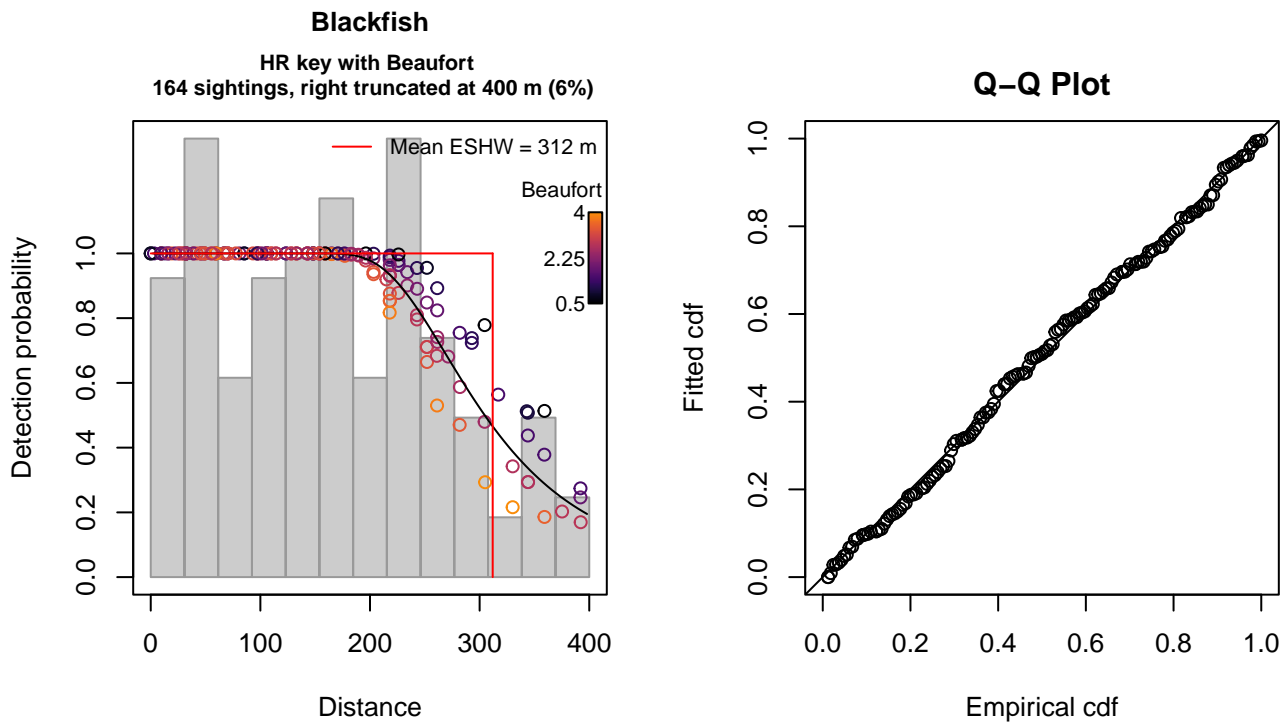
Figure 4: NEFSC AMAPPS Protocol detection function and Q-Q plot showing its goodness of fit.

Statistical output for this detection function:

```
Summary for ds object
Number of observations :  164
Distance range         :  0  -  400
AIC                    :  1943.903

Detection function:
 Hazard-rate key function

Detection function parameters
```

```
Scale coefficient(s):
             estimate          se
(Intercept)  5.85716562 0.18022637
Beaufort    -0.09331802 0.07079169


Shape coefficient(s):
          estimate          se
(Intercept)  1.49927 0.3557806


                       Estimate          SE          CV
Average p             0.7768428  0.04359073 0.05611268
N in covered region 211.1109209 14.20480094 0.06728596


Distance sampling Cramer-von Mises test (unweighted)
Test statistic = 0.038316  p = 0.941631
```
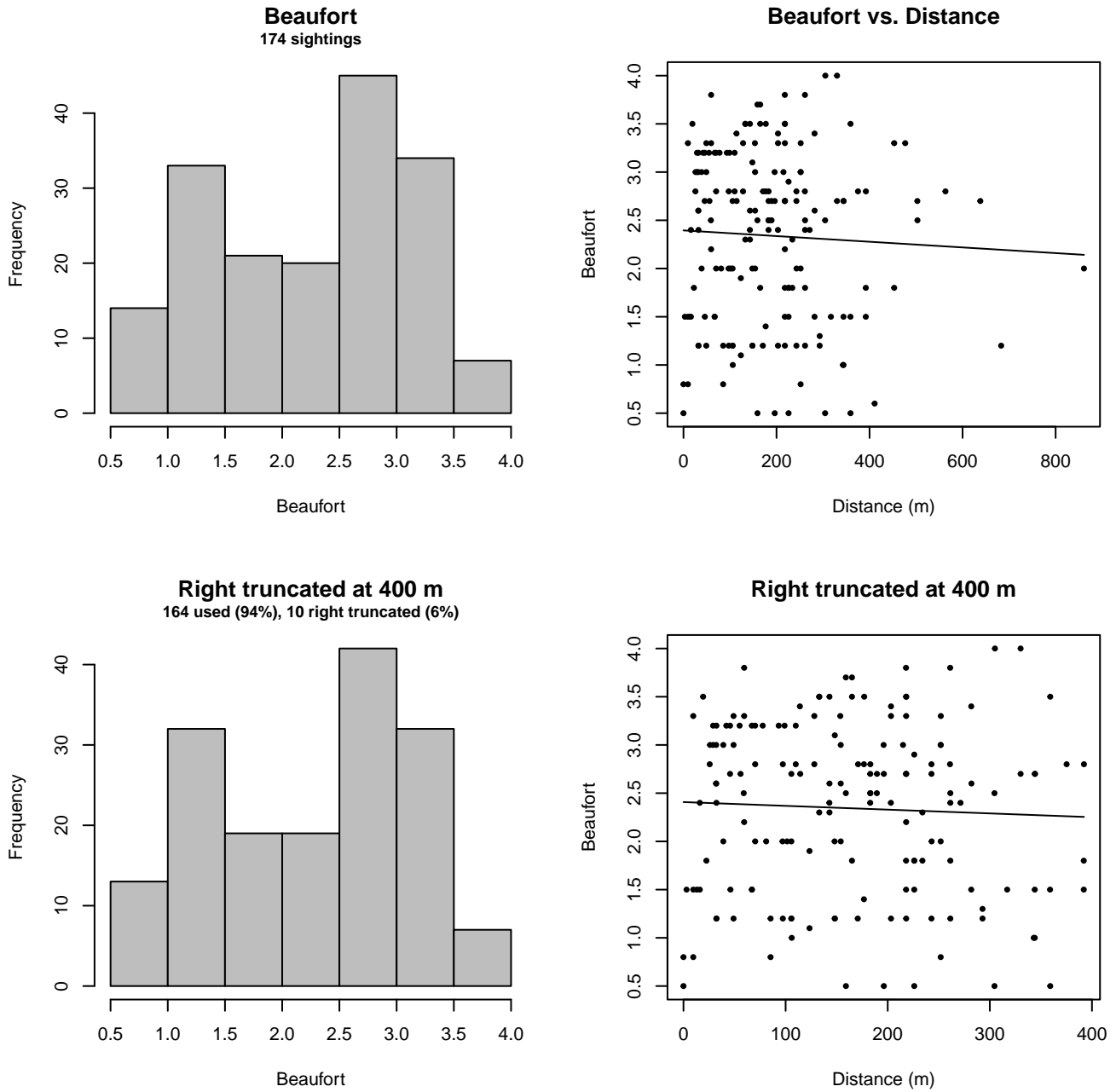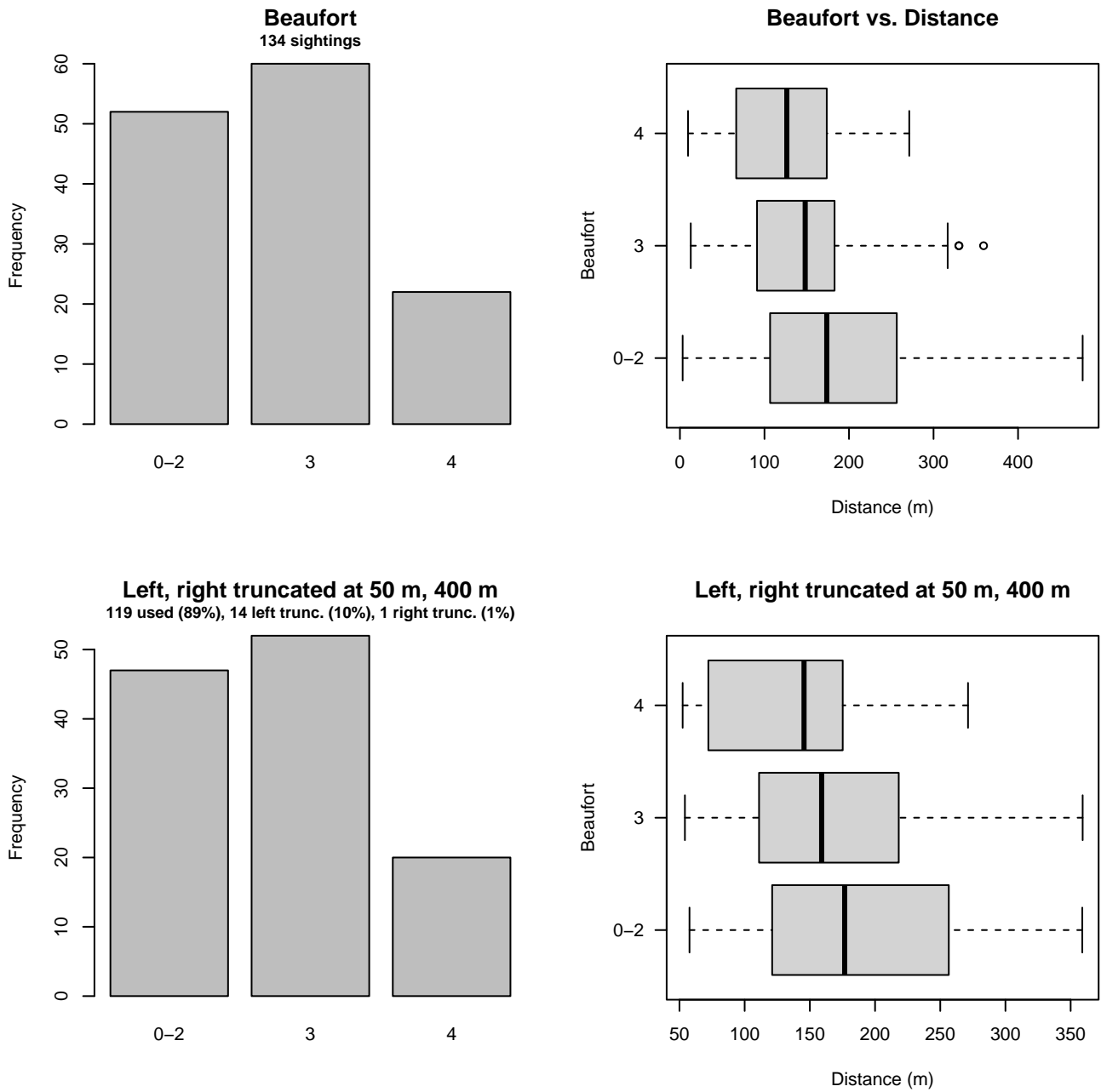
Figure 5: Distribution of the Beaufort covariate before (top row) and after (bottom row) observations were truncated to fit the NEFSC AMAPPS Protocol detection function.

2.1.1.3 SEFSC AMAPPS

After right-truncating observations greater than 400 m and left-truncating observations less than 50 m (Figure 7), we fitted the detection function to the 119 observations that remained (Table 6). The selected detection function (Figure 6) used a hazard rate key function with Beaufort (Figure 8) as a covariate.

Table 6: Observations used to fit the SEFSC AMAPPS detection function.

ScientificName	n
Globicephala	66
Grampus griseus	53
Total	**119**

11
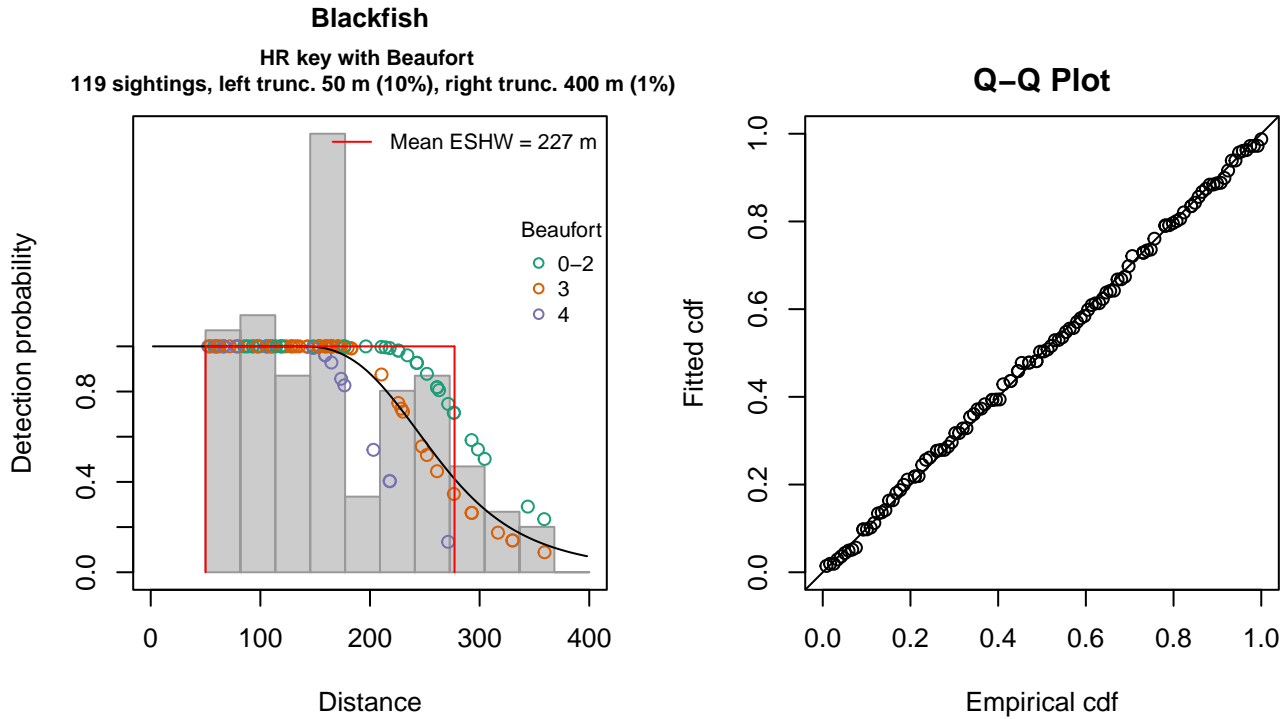
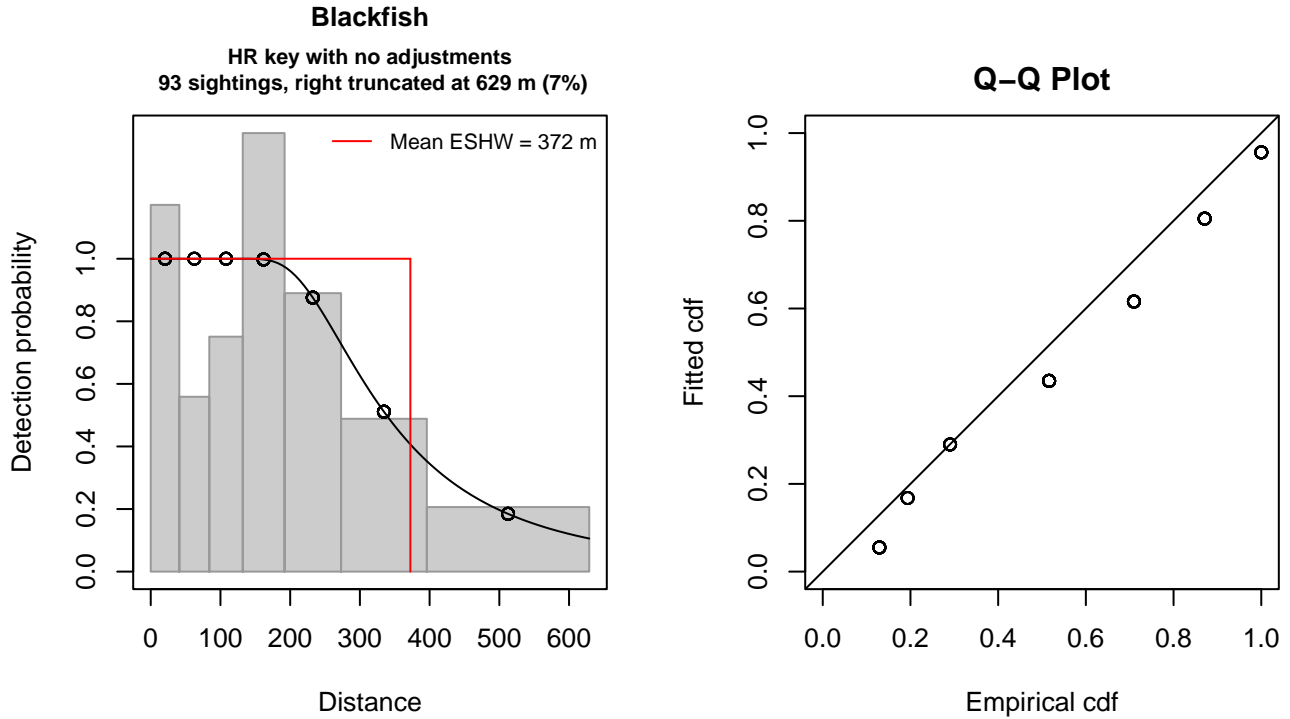Figure 6: SEFSC AMAPPS detection function and Q-Q plot showing its goodness of fit.

Statistical output for this detection function:

```
Summary for ds object
Number of observations :   119
Distance range         :   50  -   400
AIC                    :   1349.888

Detection function:
 Hazard-rate key function

Detection function parameters
Scale coefficient(s):
              estimate         se
(Intercept)  5.6569520  0.1026861
Beaufort3   -0.1814855  0.1309136
Beaufort4   -0.3857171  0.1640754

Shape coefficient(s):
            estimate        se
(Intercept) 1.761805  0.3262538

                    Estimate         SE          CV
Average p           0.6336189  0.04206604  0.06639012
N in covered region 187.8100597 16.38859266 0.08726153

Distance sampling Cramer-von Mises test (unweighted)
Test statistic = 0.019109  p = 0.997756
```

Left trucated sightings (in red)

119 used (89%), 14 left trunc. (10%), 1 right trunc. (1%)
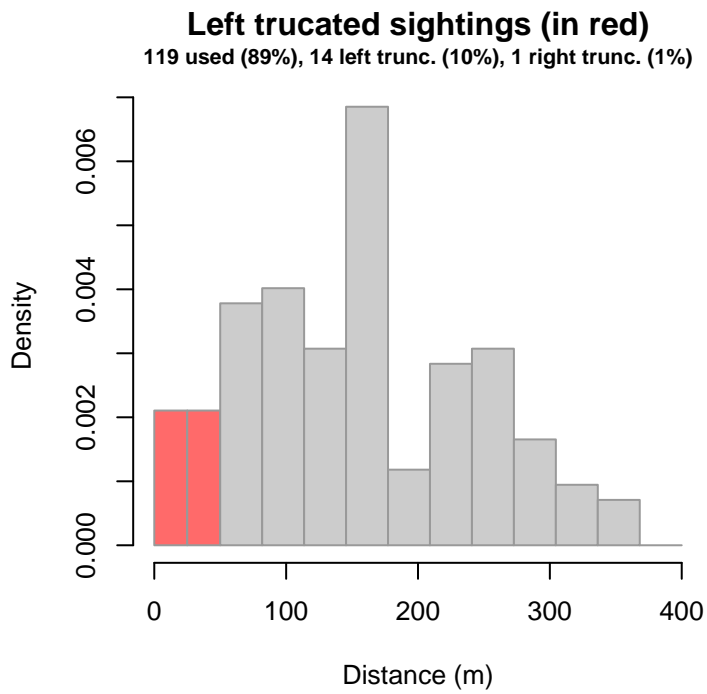
Figure 7: Density histogram of observations used to fit the SEFSC AMAPPS detection function, with the left-most bar showing observations at distances less than 50 m, which were left-truncated and excluded from the analysis [Buckland et al. (2001)]. (This bar may be very short if there were very few left-truncated sightings, or very narrow if the left truncation distance was very small; in either case it may not appear red.)

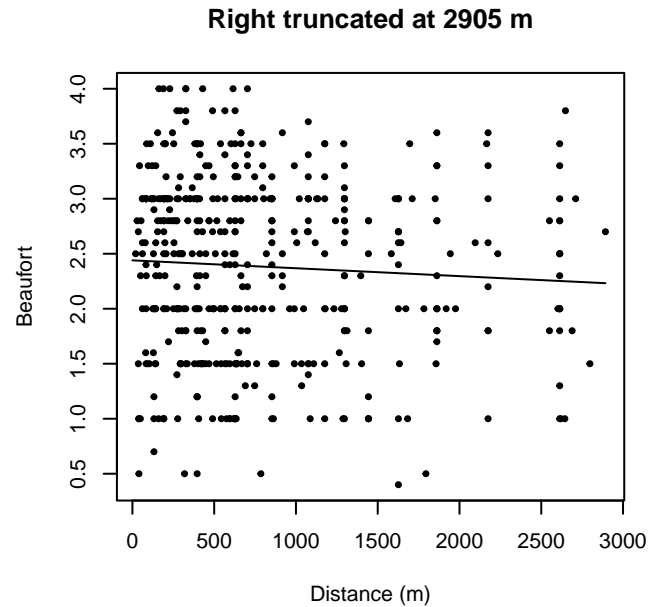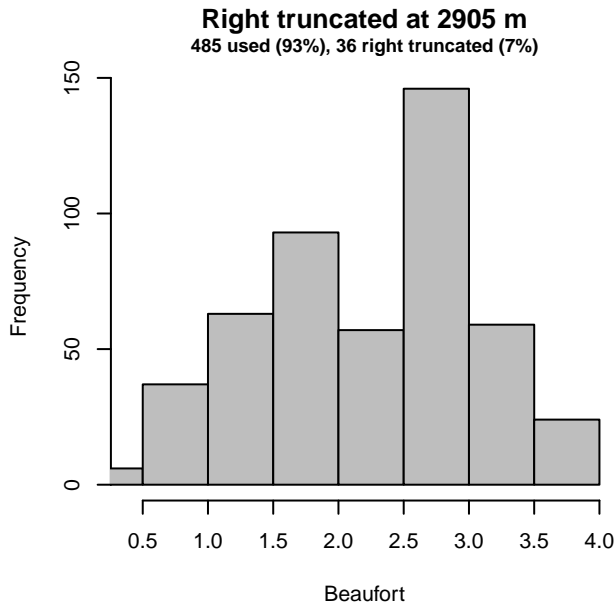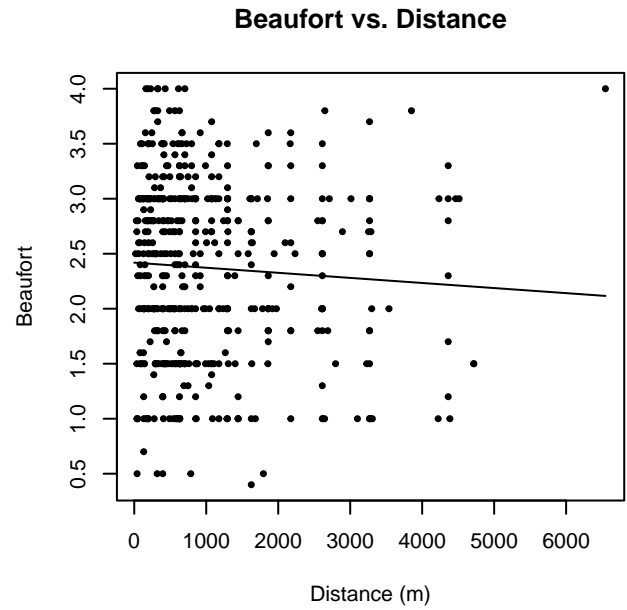Figure 8: Distribution of the Beaufort covariate before (top row) and after (bottom row) observations were truncated to fit the SEFSC AMAPPS detection function.

2.1.1.4 750 ft

After right-truncating observations greater than 629 m, we fitted the detection function to the 93 observations that remained (Table 7). The selected detection function (Figure 9) used a hazard rate key function with no covariates.

Table 7: Observations used to fit the 750 ft detection function.

ScientificName	n
Feresa attenuata	3
Feresa attenuata/Peponocephala electra	7
Globicephala	12
Grampus griseus	69
Pseudorca crassidens	2
Total	**93**

Figure 9: 750 ft detection function and Q-Q plot showing its goodness of fit.

Statistical output for this detection function:

```
Summary for ds object
Number of observations :  93
Distance range        :  0  -  629
AIC                   :  359.4726

Detection function:
 Hazard-rate key function

Detection function parameters
Scale coefficient(s):
          estimate        se
(Intercept) 5.698811 0.1702564

Shape coefficient(s):
          estimate        se
(Intercept)  1.07856 0.3654486

                Estimate         SE        CV
Average p      0.5920954  0.06138719 0.1036779
```

15

```
N in covered region  157.0692704  19.32345801  0.1230251
```

```
Distance sampling Cramer-von Mises test (unweighted)
Test statistic = 0.271977  p = 0.162483
```
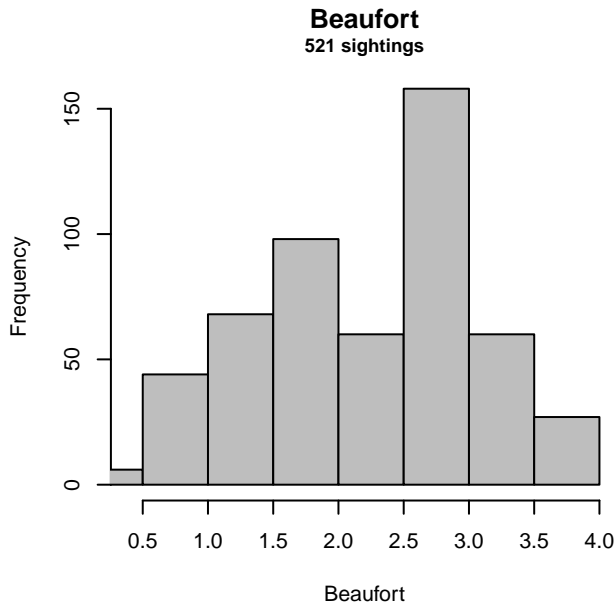
2.1.1.5 NARWSS 2003-2016

After right-truncating observations greater than 2905 m, we fitted the detection function to the 485 observations that remained (Table 8). The selected detection function (Figure 10) used a hazard rate key function with Beaufort (Figure 11) as a covariate.

Table 8: Observations used to fit the NARWSS 2003-2016 detection function.

| ScientificName	n
Globicephala	376
Grampus griseus	106
Orcinus orca	3
Total	**485**
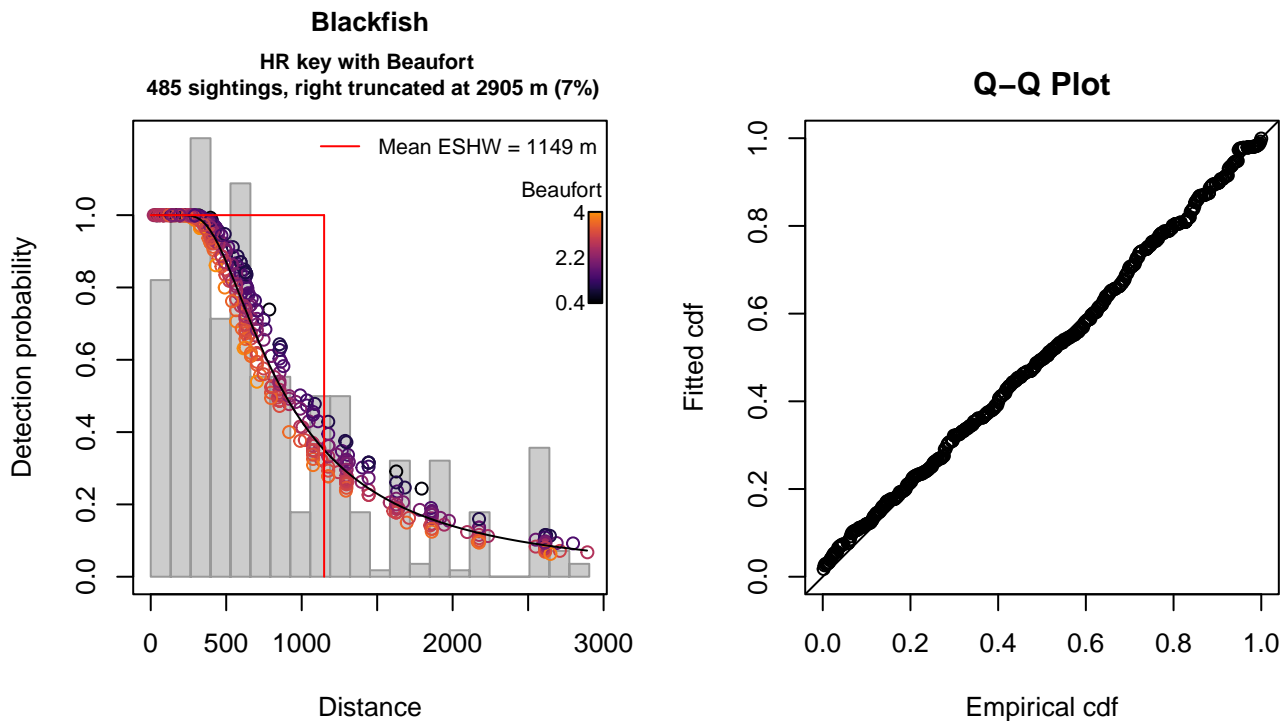
Figure 10: NARWSS 2003-2016 detection function and Q-Q plot showing its goodness of fit.

Statistical output for this detection function:

```
Summary for ds object
Number of observations :  485
Distance range         :  0  -  2905
AIC                    :  7420.46

Detection function:
 Hazard-rate key function

Detection function parameters
Scale coefficient(s):
```

```
                estimate         se
(Intercept)   6.8787415 0.22789350
Beaufort     -0.1141738 0.08537414


Shape coefficient(s):
              estimate         se
(Intercept) 0.6421837 0.09908371


                         Estimate          SE         CV
Average p                0.393189  0.02454407 0.06242307
N in covered region 1233.503530 88.54090900 0.07178002


Distance sampling Cramer-von Mises test (unweighted)
Test statistic = 0.097833  p = 0.595605
```

Figure 11: Distribution of the Beaufort covariate before (top row) and after (bottom row) observations were truncated to fit the NARWSS 2003-2016 detection function.

2.1.1.6 NEAq New England

After right-truncating observations greater than 1852 m and left-truncating observations less than 71 m (Figure 13), we fitted the detection function to the 58 observations that remained (Table 9). The selected detection function (Figure 12) used a half normal key function with no covariates.

Table 9: Observations used to fit the NEAq New England detection function.

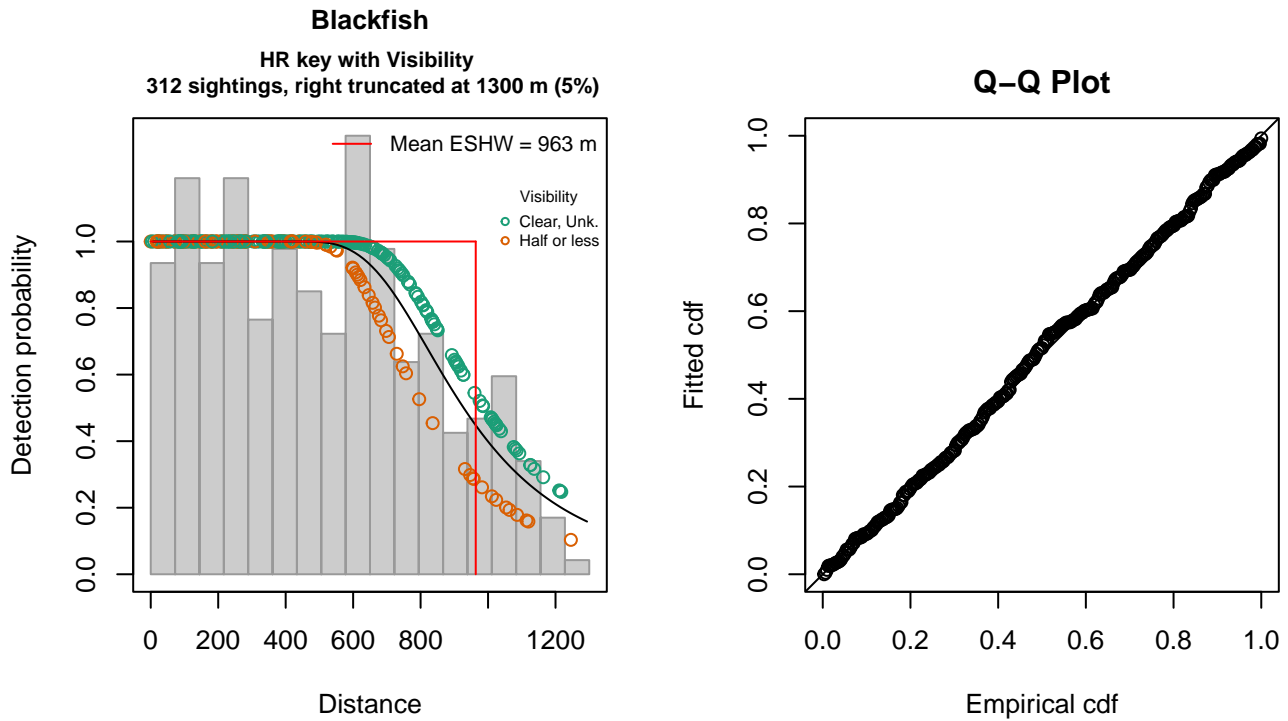| ScientificName	n
Globicephala	16
Grampus griseus	42
Total	**58**
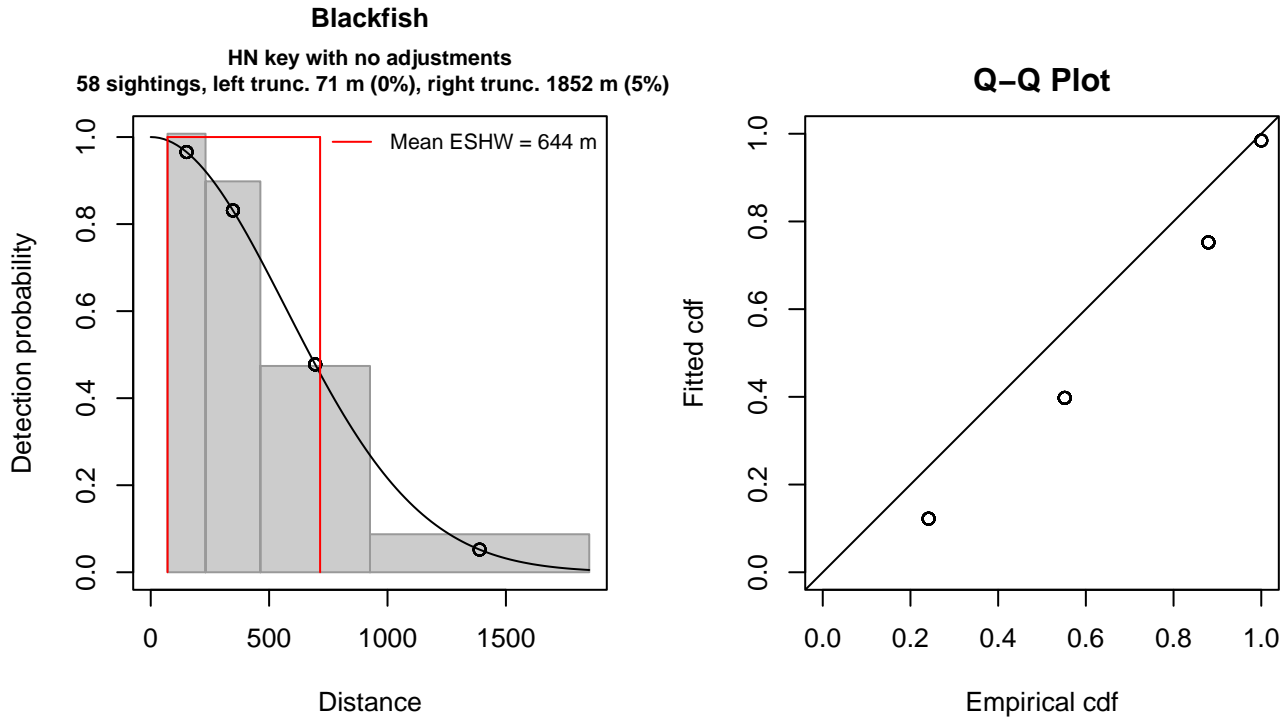
Figure 12: NEAq New England detection function and Q-Q plot showing its goodness of fit.

Statistical output for this detection function:

```
Summary for ds object
Number of observations :   58
Distance range         :   71  -  1852
AIC                    :   156.0466

Detection function:
 Half-normal key function

Detection function parameters
Scale coefficient(s):
            estimate           se
(Intercept) 6.347853 0.1032999


                     Estimate          SE         CV
Average p           0.3617668  0.04089634 0.1130461
N in covered region 160.3242530 24.72501947 0.1542188

Distance sampling Cramer-von Mises test (unweighted)
Test statistic = 0.430759  p = 0.060002
```

Left trucated sightings (in red)

58 used (95%), 0 left trunc. (0%), 3 right trunc. (5%)
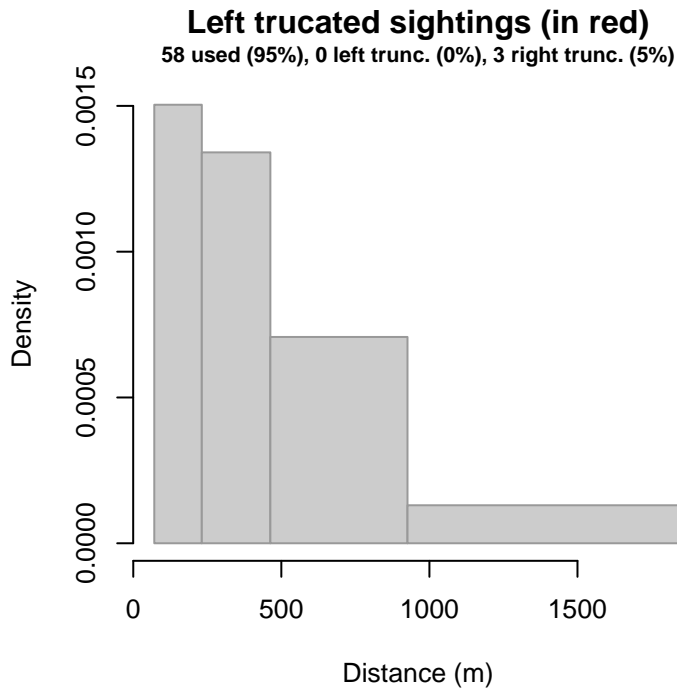
Figure 13: Density histogram of observations used to fit the NEAq New England detection function, with the left-most bar showing observations at distances less than 71 m, which were left-truncated and excluded from the analysis [Buckland et al. (2001)]. (This bar may be very short if there were very few left-truncated sightings, or very narrow if the left truncation distance was very small; in either case it may not appear red.)

2.1.1.7 UNCW Navy and VAMSC

After right-truncating observations greater than 1300 m, we fitted the detection function to the 312 observations that remained (Table 10). The selected detection function (Figure 14) used a hazard rate key function with Visibility (Figure 15) as a covariate.

Table 10: Observations used to fit the UNCW Navy and VAMSC detection function.

| ScientificName	n
Globicephala macrorhynchus	223
Grampus griseus	88
Peponocephala electra	1
Total	**312**

Figure 14: UNCW Navy and VAMSC detection function and Q-Q plot showing its goodness of fit.

Statistical output for this detection function:

```
Summary for ds object
Number of observations :  312
Distance range         :  0  -  1300
AIC                    :  4410.896

Detection function:
 Hazard-rate key function

Detection function parameters
Scale coefficient(s):
                        estimate          se
(Intercept)            6.8110764  0.06588732
VisibilityHalf or less -0.1997402 0.10267594

Shape coefficient(s):
            estimate         se
(Intercept)  1.45681  0.2585487


                      Estimate         SE         CV
Average p            0.7368436  0.03057513 0.04149473
N in covered region 423.4277360 21.50283164 0.05078277


Distance sampling Cramer-von Mises test (unweighted)
Test statistic = 0.030099  p = 0.975843
```
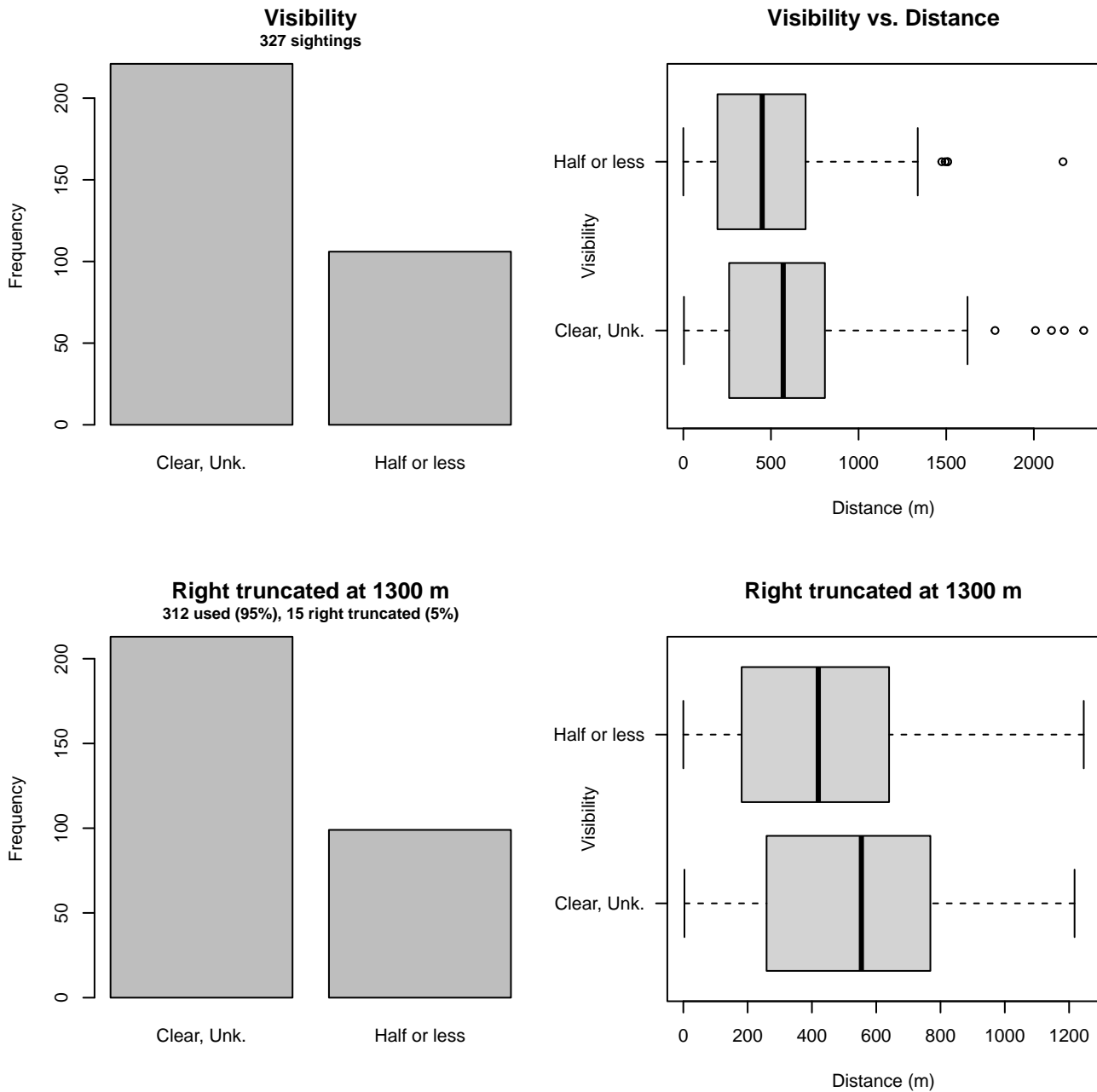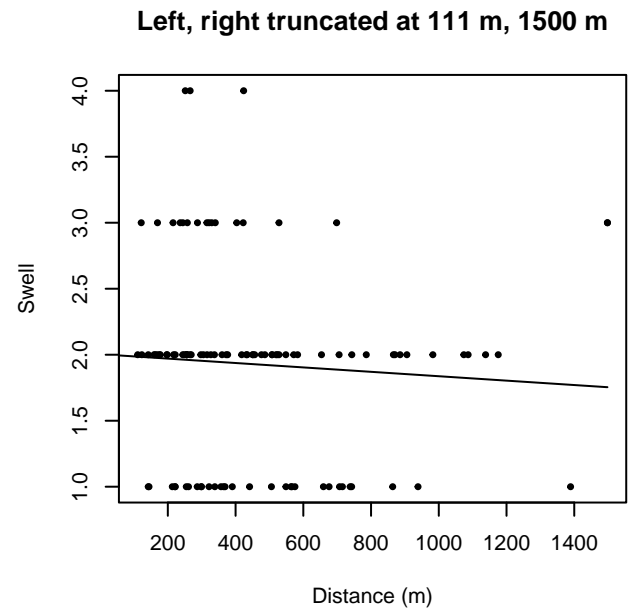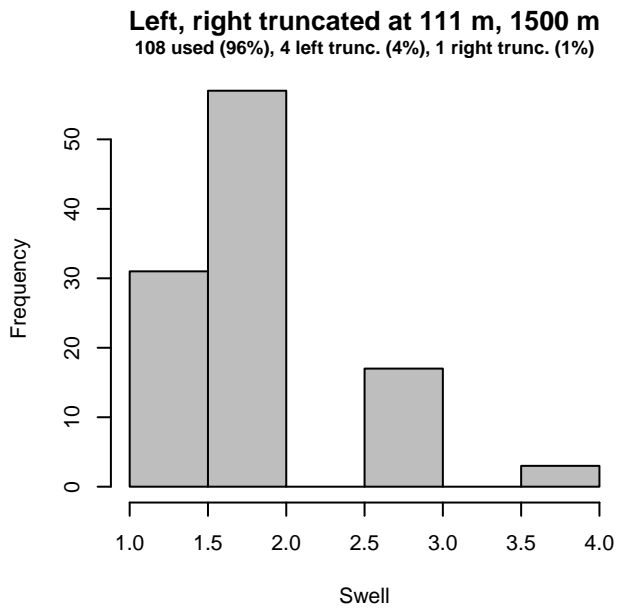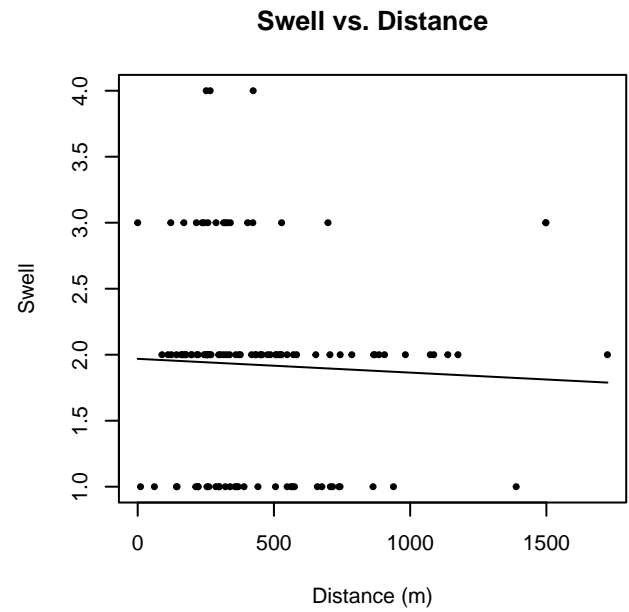
Figure 15: Distribution of the Visibility covariate before (top row) and after (bottom row) observations were truncated to fit the UNCW Navy and VAMSC detection function.

2.1.1.8 HDR

After right-truncating observations greater than 1500 m and left-truncating observations less than 111 m (Figure 17), we fitted the detection function to the 108 observations that remained (Table 11). The selected detection function (Figure 16) used a hazard rate key function with Swell (Figure 18) as a covariate.

Table 11: Observations used to fit the HDR detection function.

ScientificName	n
Globicephala	66
Grampus griseus	42
Total	**108**
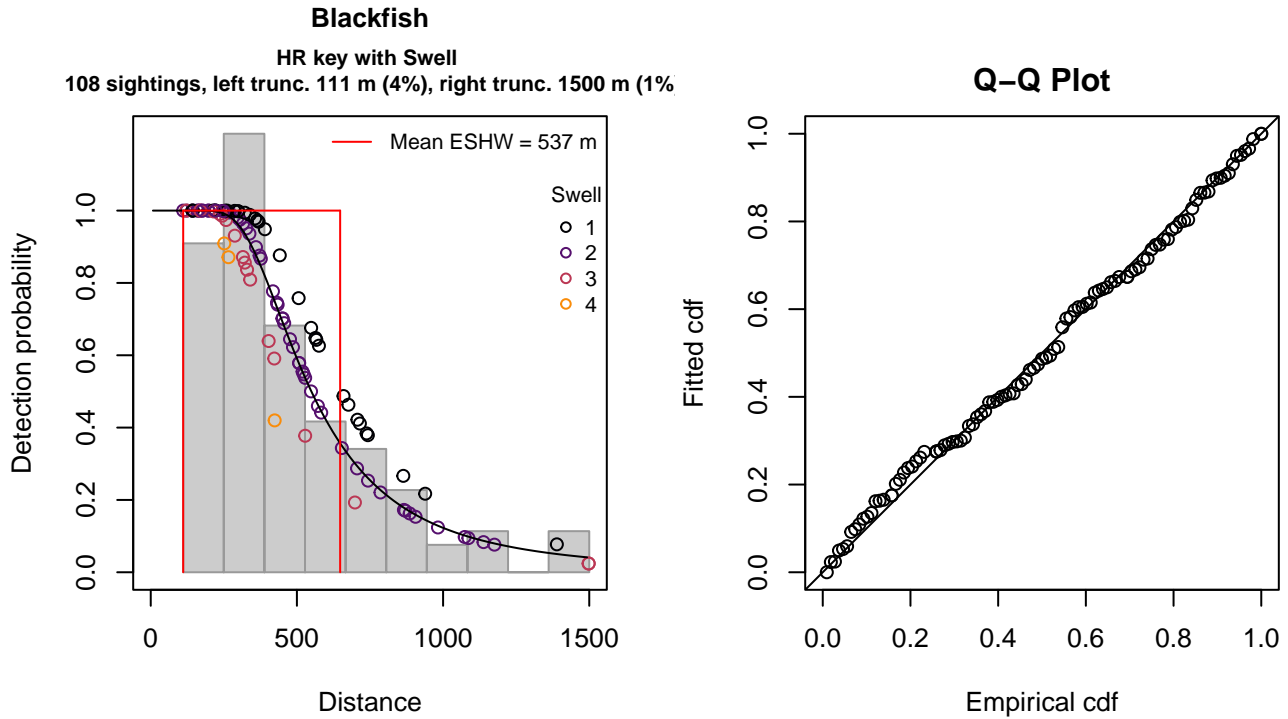
Figure 16: HDR detection function and Q-Q plot showing its goodness of fit.

Statistical output for this detection function:

```
Summary for ds object
Number of observations :   108
Distance range         :   111  -  1500
AIC                    :   1479.102

Detection function:
 Hazard-rate key function

Detection function parameters
Scale coefficient(s):
             estimate         se
(Intercept)  6.5207075 0.2852850
Swell       -0.1712662 0.1474231

Shape coefficient(s):
            estimate          se
(Intercept) 1.044626 0.1820091


                      Estimate         SE          CV
Average p            0.3789427  0.04750114 0.1253518
N in covered region 285.0035382 41.82280744 0.1467449

Distance sampling Cramer-von Mises test (unweighted)
Test statistic = 0.045799  p = 0.901252
```

Left trucated sightings (in red)

108 used (96%), 4 left trunc. (4%), 1 right trunc. (1%)
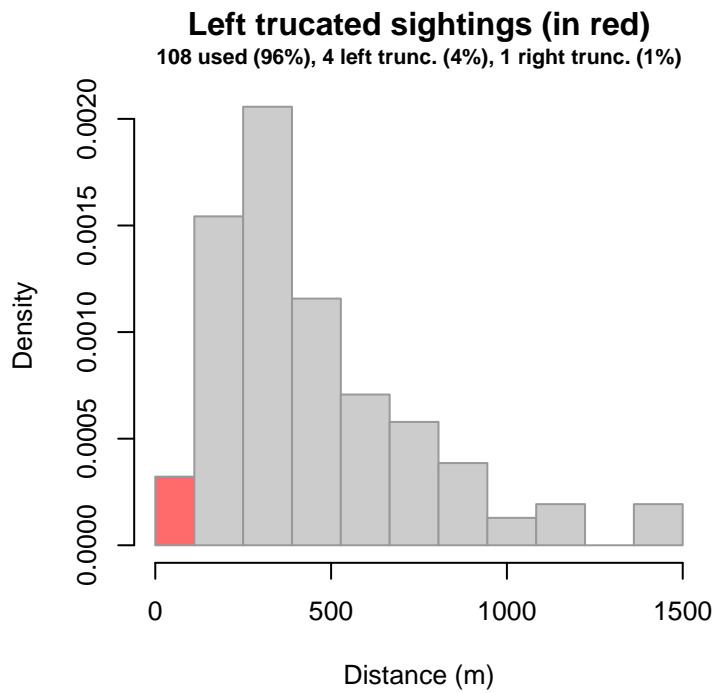
Figure 17: Density histogram of observations used to fit the HDR detection function, with the left-most bar showing observations at distances less than 111 m, which were left-truncated and excluded from the analysis [Buckland et al. (2001)]. (This bar may be very short if there were very few left-truncated sightings, or very narrow if the left truncation distance was very small; in either case it may not appear red.)
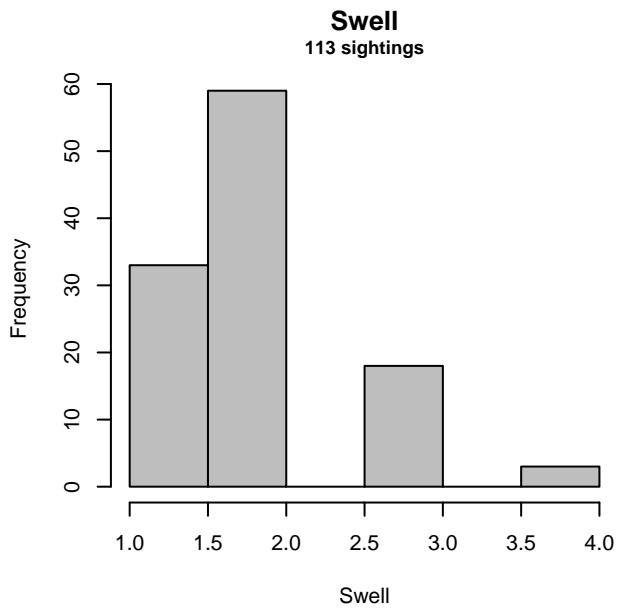
Figure 18: Distribution of the Swell covariate before (top row) and after (bottom row) observations were truncated to fit the HDR detection function.

2.1.2 Shipboard Surveys
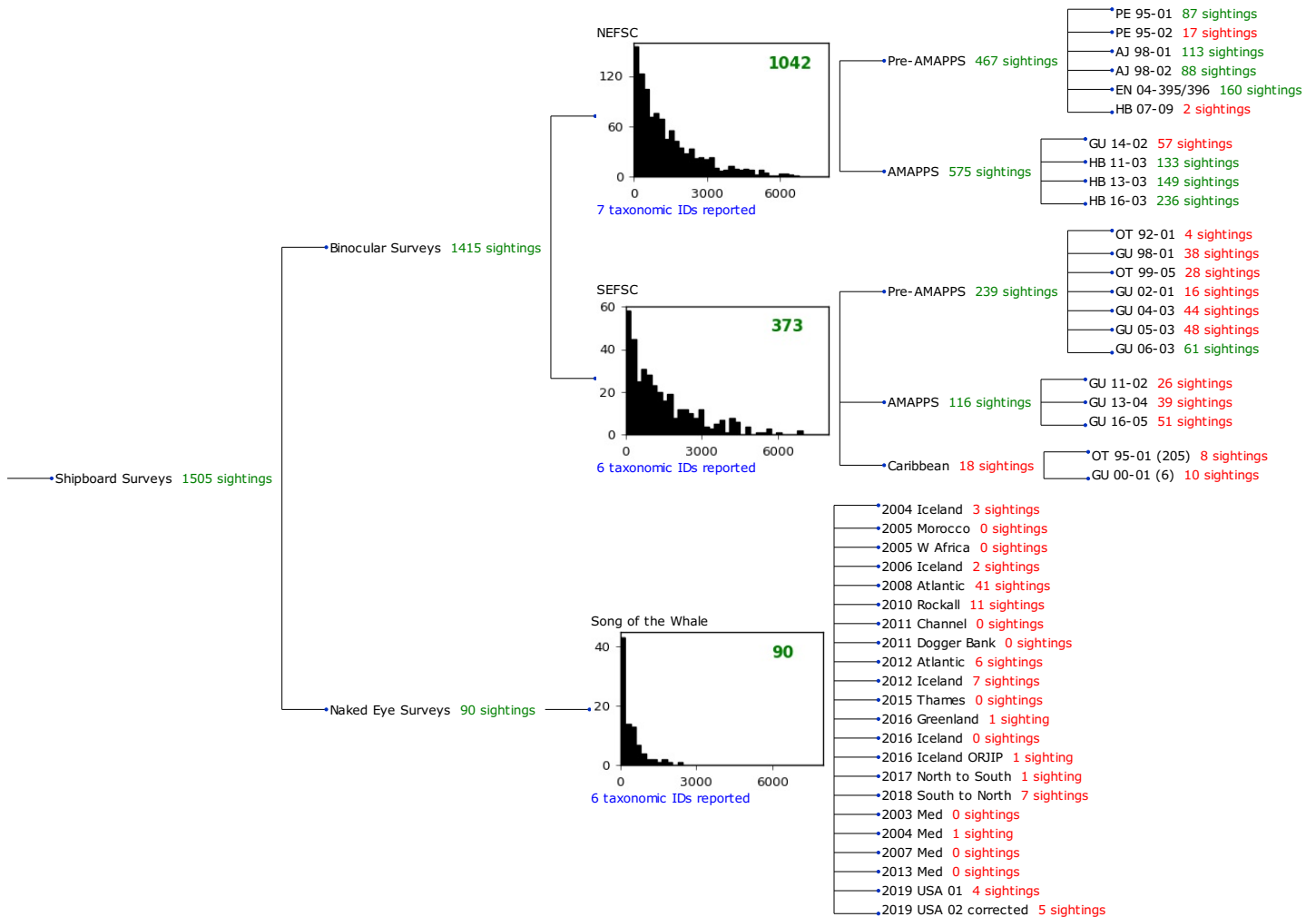
Figure 19: Detection hierarchy for shipboard surveys, showing how they were pooled during detectability modeling, for detection functions that pooled multiple taxa but could not use a taxonomic covariate to account for differences between them. Each histogram represents a detection function and summarizes the perpendicular distances of observations that were pooled to fit it, prior to truncation. Observation counts, also prior to truncation, are shown in green when they met the recommendation of Buckland et al. (2001) that detection functions utilize at least 60 sightings, and red otherwise. For rare taxa, it was not always possible to meet this recommendation, yielding higher statistical uncertainty. During the spatial modeling stage of the analysis, effective strip widths were computed for each survey using the closest detection function above it in the hierarchy (i.e. moving from right to left in the figure). Surveys that do not have a detection function above them in this figure were either addressed by a detection function presented in a different section of this report, or were omitted from the analysis.

2.1.2.1 NEFSC

After right-truncating observations greater than 6500 m, we fitted the detection function to the 1038 observations that remained (Table 12). The selected detection function (Figure 20) used a hazard rate key function with Beaufort (Figure 21), Program (Figure 22) and VesselName (Figure 23) as covariates.

Table 12: Observations used to fit the NEFSC detection function.

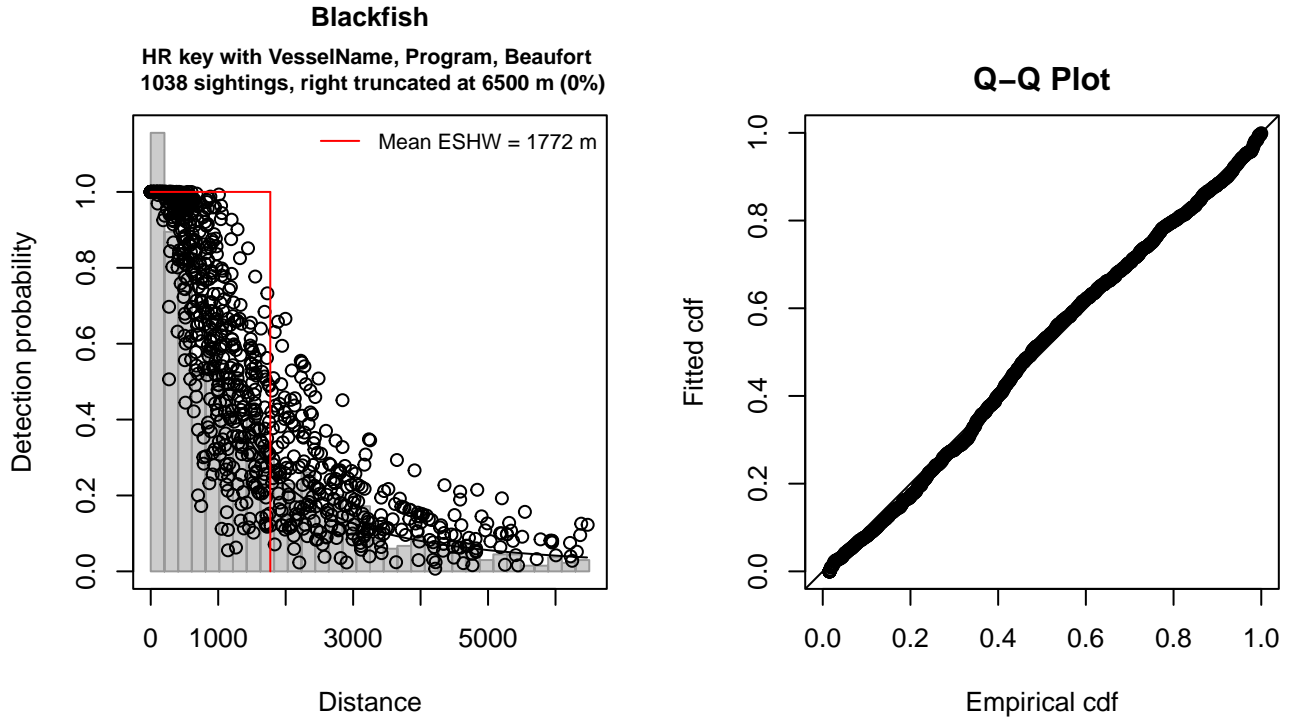| ScientificName	n
Feresa attenuata	1
Globicephala	339
Globicephala macrorhynchus	3
Globicephala melas	2
Grampus griseus	687
Orcinus orca	2
Pseudorca crassidens	4
Total	**1038**

Figure 20: NEFSC detection function and Q-Q plot showing its goodness of fit.

Statistical output for this detection function:

```
Summary for ds object
Number of observations :  1038
Distance range         :  0  -  6500
AIC                    :  17099.06

Detection function:
 Hazard-rate key function

Detection function parameters
Scale coefficient(s):
                                         estimate          se
(Intercept)                             7.9293942 0.15761667
VesselNameGunter                       -0.8354128 0.20812306
VesselNamePelican                      -0.3342984 0.17874334
ProgramMarine Mammal Abundance Surveys -0.2436275 0.10871377
Beaufort                               -0.3461133 0.05534466
```

```
Shape coefficient(s):
             estimate            se
(Intercept) 0.5332413 0.05606824


                      Estimate          SE          CV
Average p            0.2418497    0.01240714 0.05130104
N in covered region 4291.9212516 249.96005128 0.05823966


Distance sampling Cramer-von Mises test (unweighted)
Test statistic = 0.293125   p = 0.141354
```
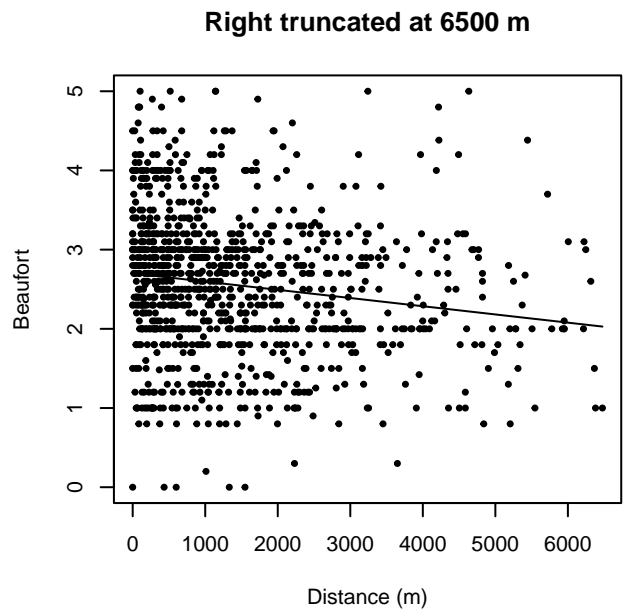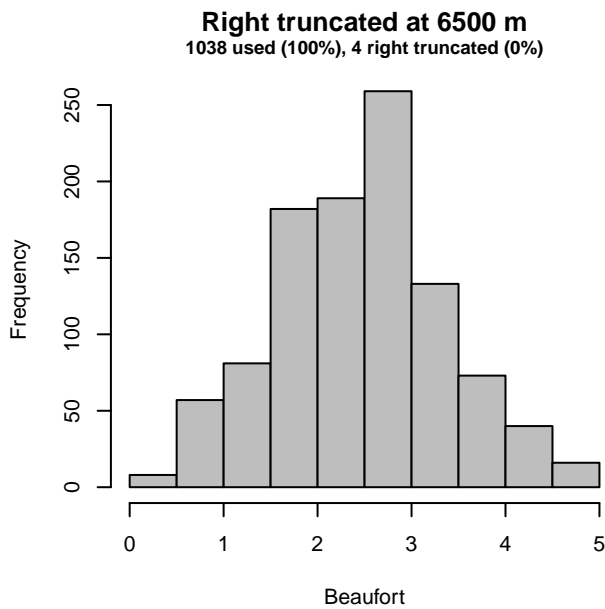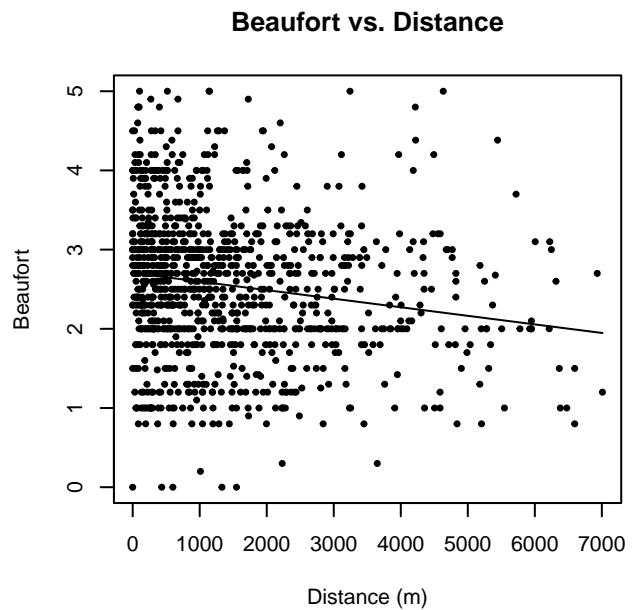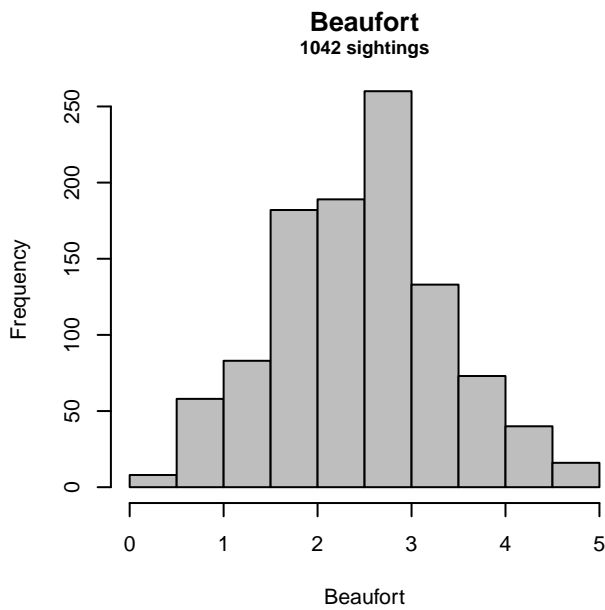

Figure 21: Distribution of the Beaufort covariate before (top row) and after (bottom row) observations were truncated to fit the NEFSC detection function.
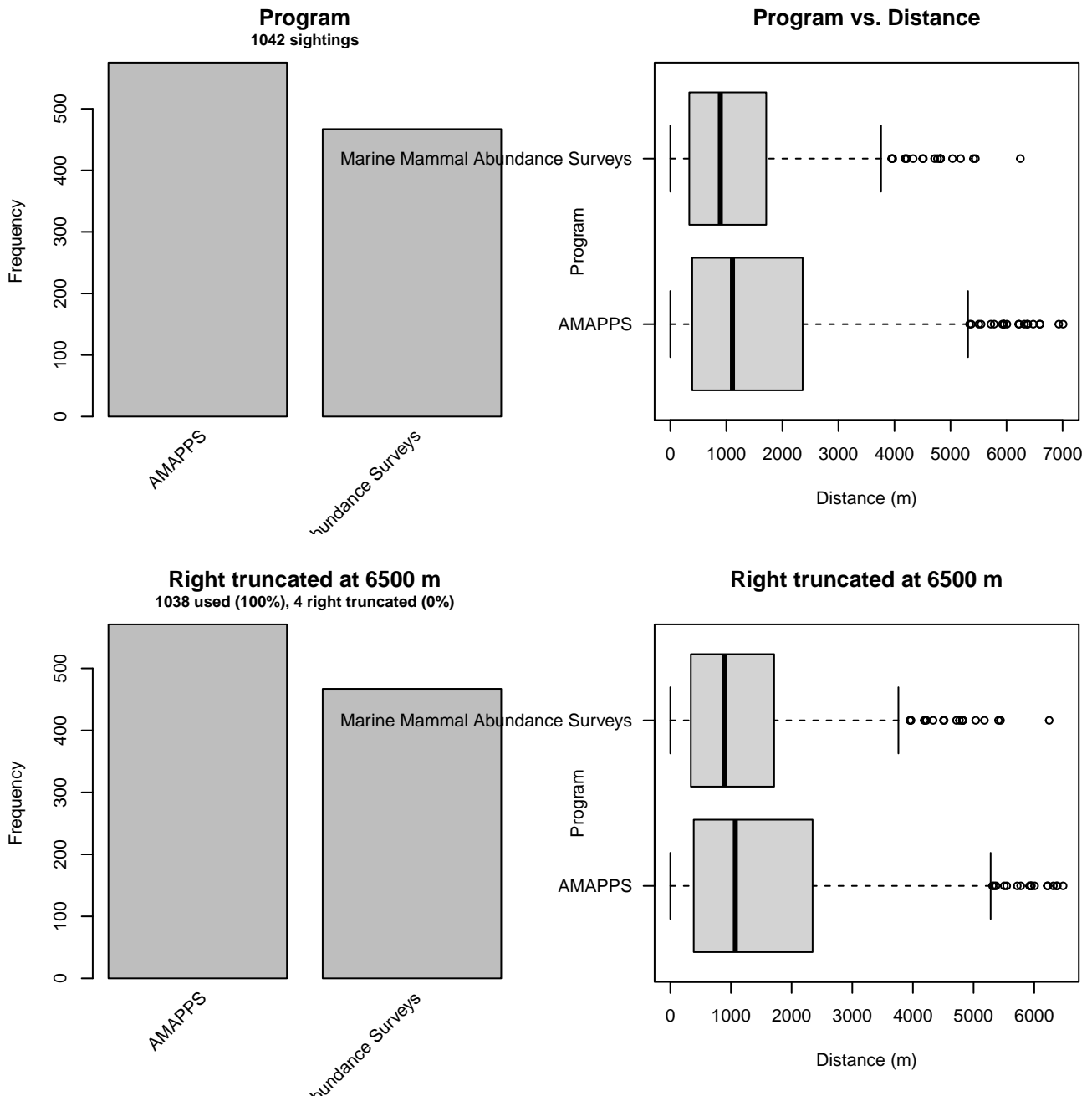
Figure 22: Distribution of the Program covariate before (top row) and after (bottom row) observations were truncated to fit the NEFSC detection function.
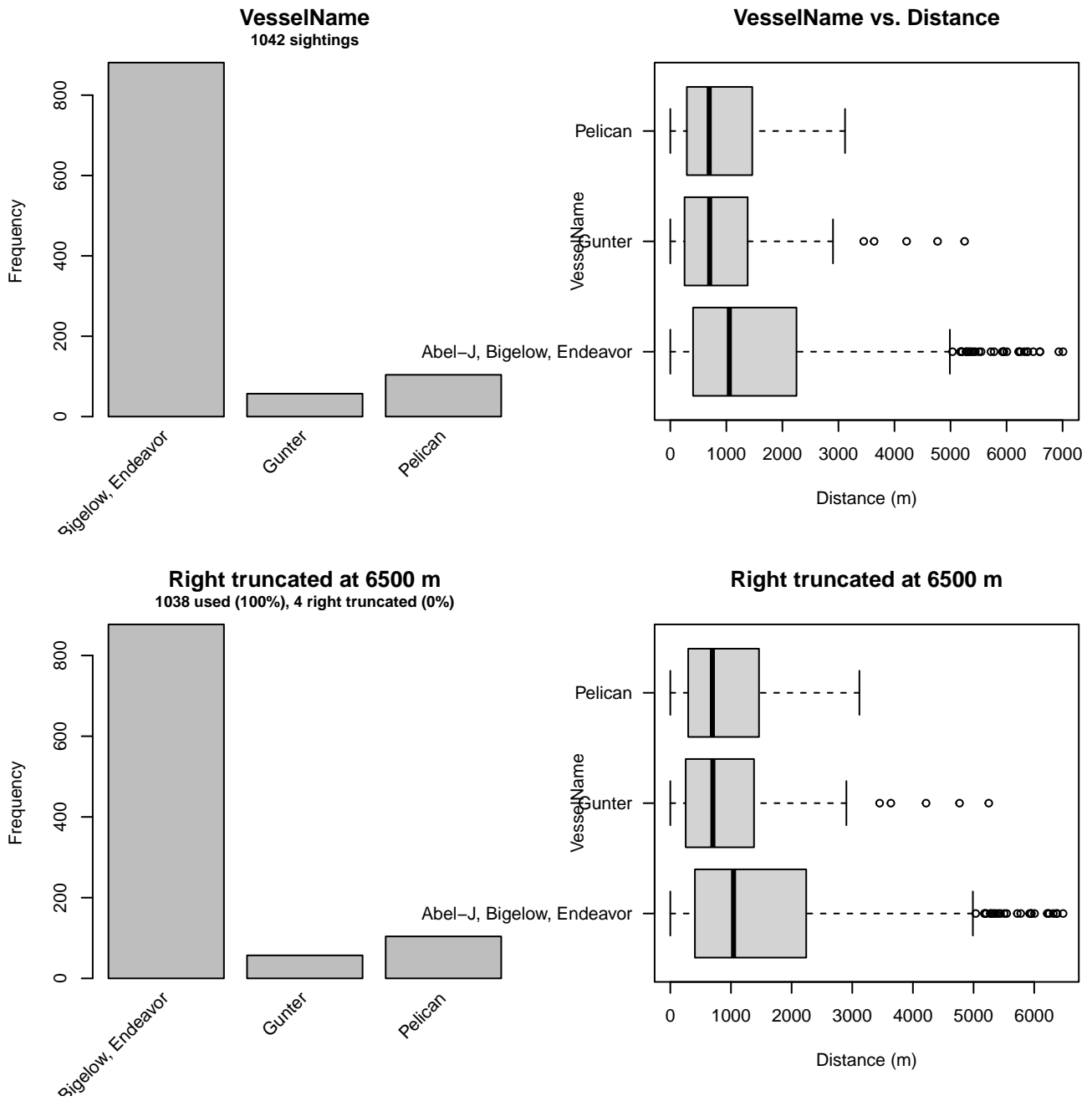
Figure 23: Distribution of the VesselName covariate before (top row) and after (bottom row) observations were truncated to fit the NEFSC detection function.

2.1.2.2 SEFSC

After right-truncating observations greater than 4500 m, we fitted the detection function to the 361 observations that remained (Table 13). The selected detection function (Figure 24) used a hazard rate key function with Beaufort (Figure 25) and VesselName (Figure 26) as covariates.

Table 13: Observations used to fit the SEFSC detection function.

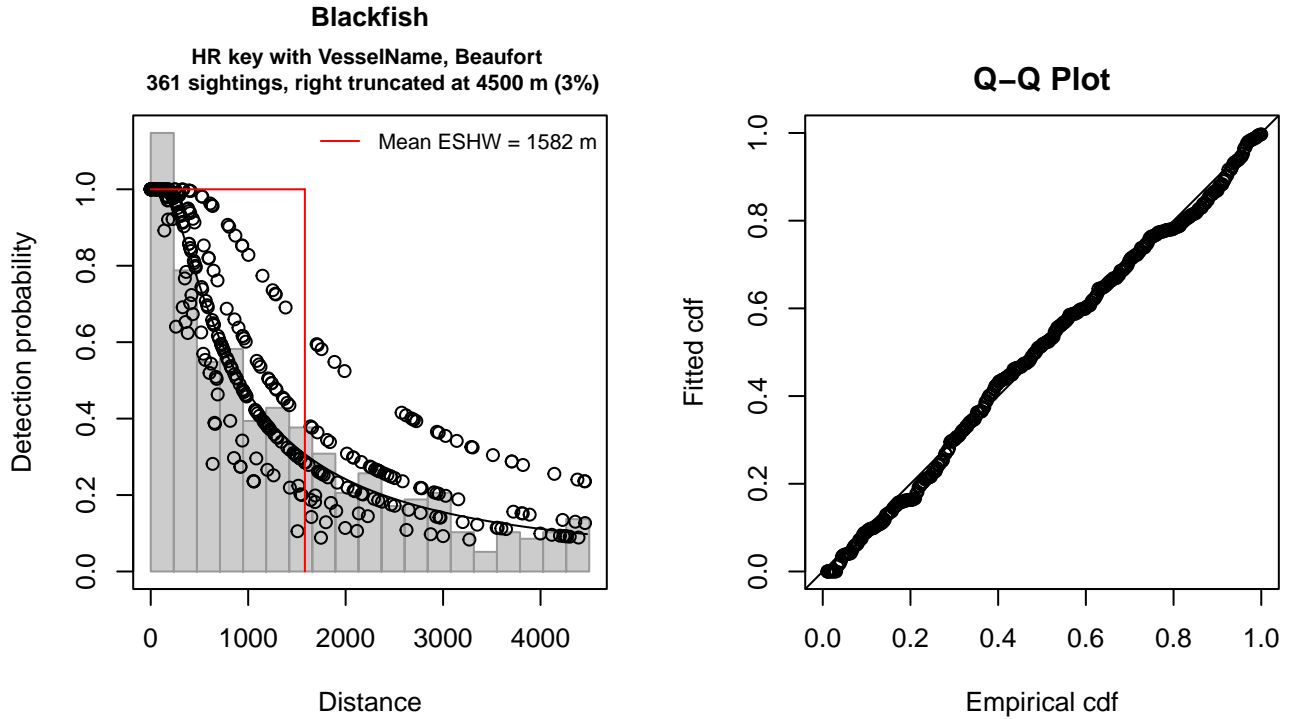| ScientificName	n
Feresa attenuata/Peponocephala electra	7
Globicephala	227
Grampus griseus	121
Orcinus orca	1
Peponocephala electra	3
Pseudorca crassidens	2
Total	**361**

Figure 24: SEFSC detection function and Q-Q plot showing its goodness of fit.

Statistical output for this detection function:

```
Summary for ds object
Number of observations :  361
Distance range         :  0  -  4500
AIC                    :  5876.279

Detection function:
 Hazard-rate key function

Detection function parameters
Scale coefficient(s):
                      estimate        se
(Intercept)          7.3597538 0.3426685
VesselNameOregon II -0.5805409 0.4158932
Beaufort2           -0.5439643 0.4011114
Beaufort3-4         -0.8577400 0.3820711
Beaufort5           -1.2038982 0.5170081

Shape coefficient(s):
```

```
                estimate          se
(Intercept) 0.2309157 0.1254747


                        Estimate          SE           CV
Average p              0.3253837    0.03477386  0.1068703
N in covered region 1109.4594048 128.24893603  0.1155959


Distance sampling Cramer-von Mises test (unweighted)
Test statistic = 0.112666  p = 0.526278
```
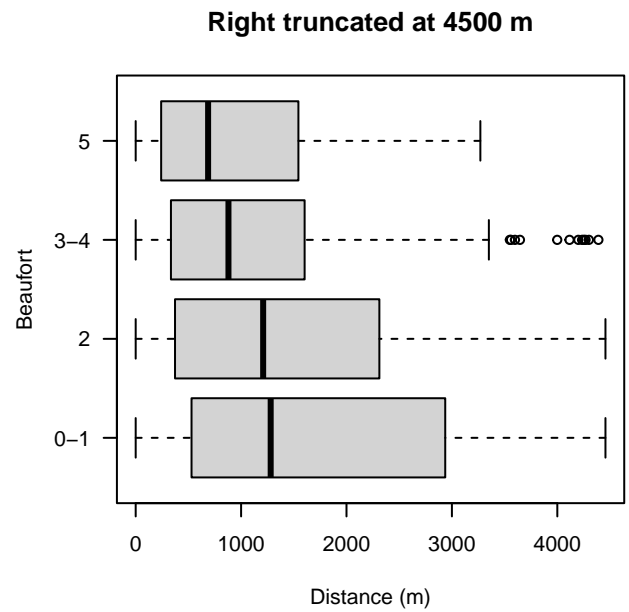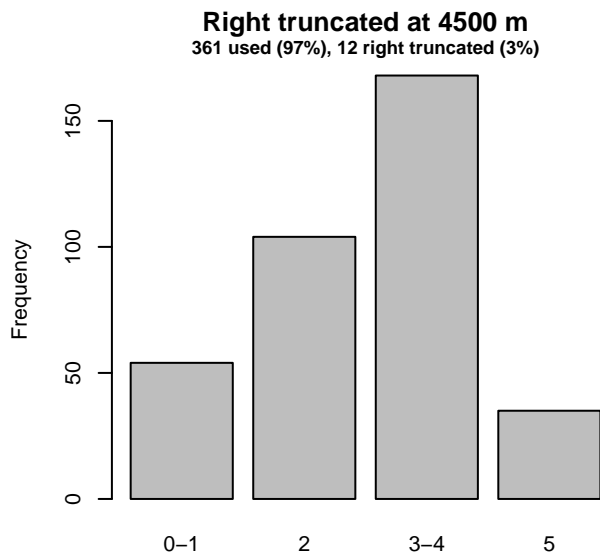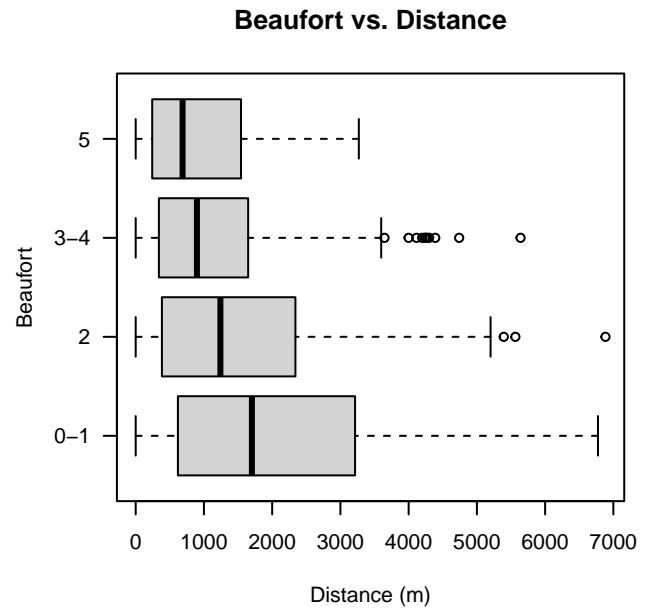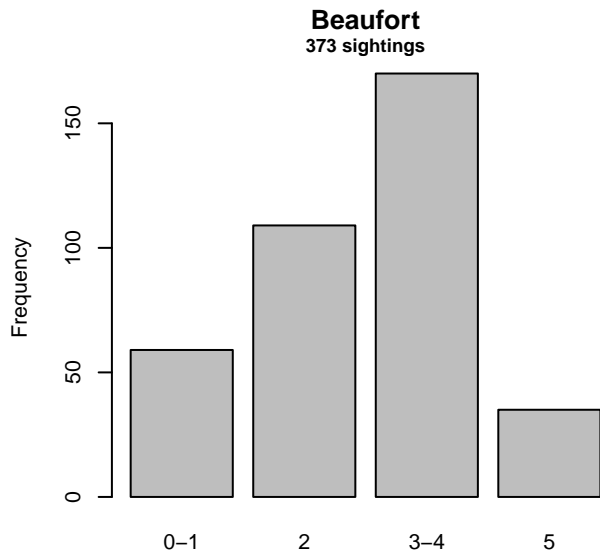

Figure 25: Distribution of the Beaufort covariate before (top row) and after (bottom row) observations were truncated to fit the SEFSC detection function.
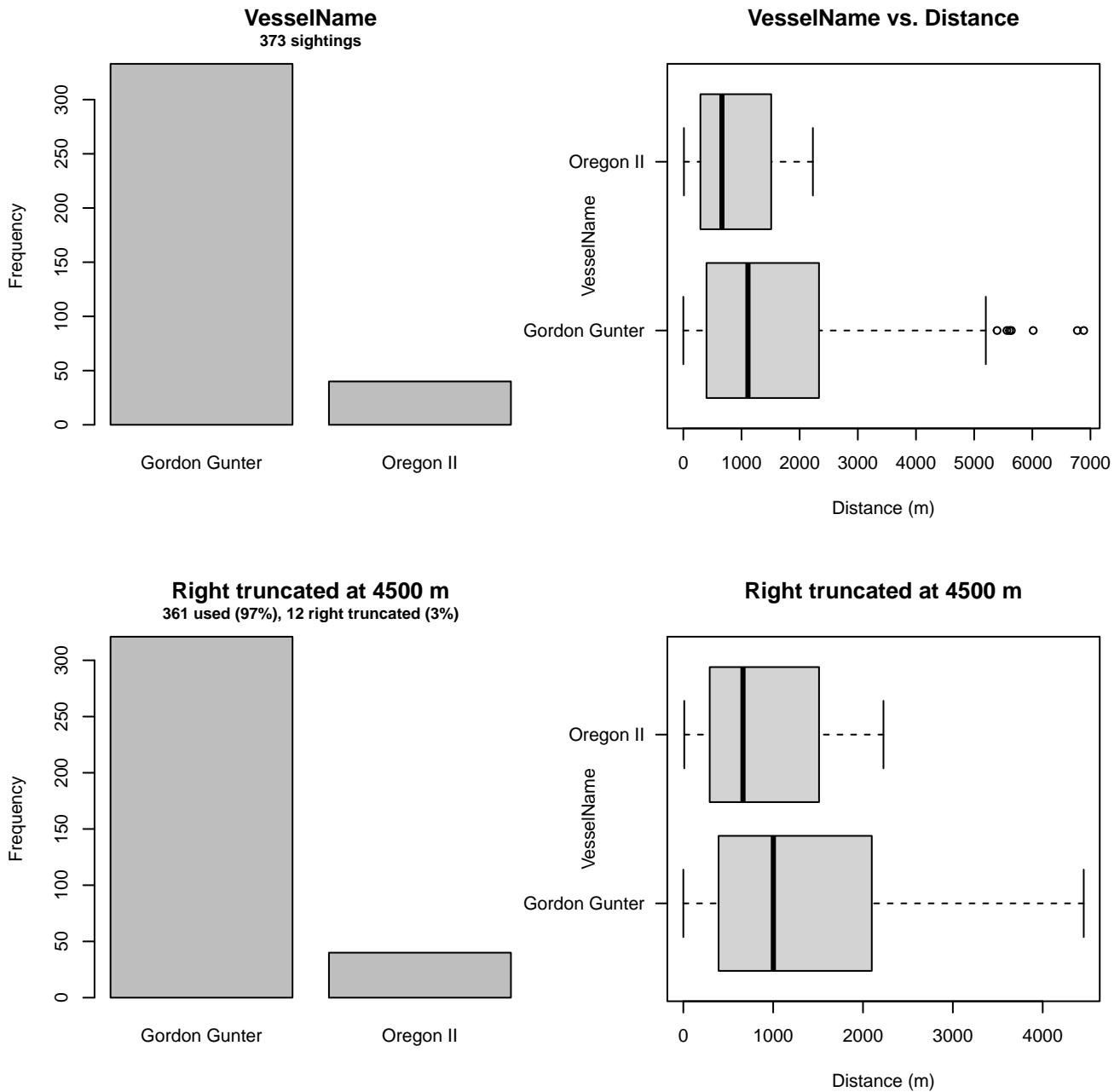
Figure 26: Distribution of the VesselName covariate before (top row) and after (bottom row) observations were truncated to fit the SEFSC detection function.

2.1.2.3 Song of the Whale

After right-truncating observations greater than 1500 m, we fitted the detection function to the 86 observations that remained (Table 14). The selected detection function (Figure 27) used a hazard rate key function with Beaufort (Figure 28) and Clouds (Figure 29) as covariates.

Table 14: Observations used to fit the Song of the Whale detection function.

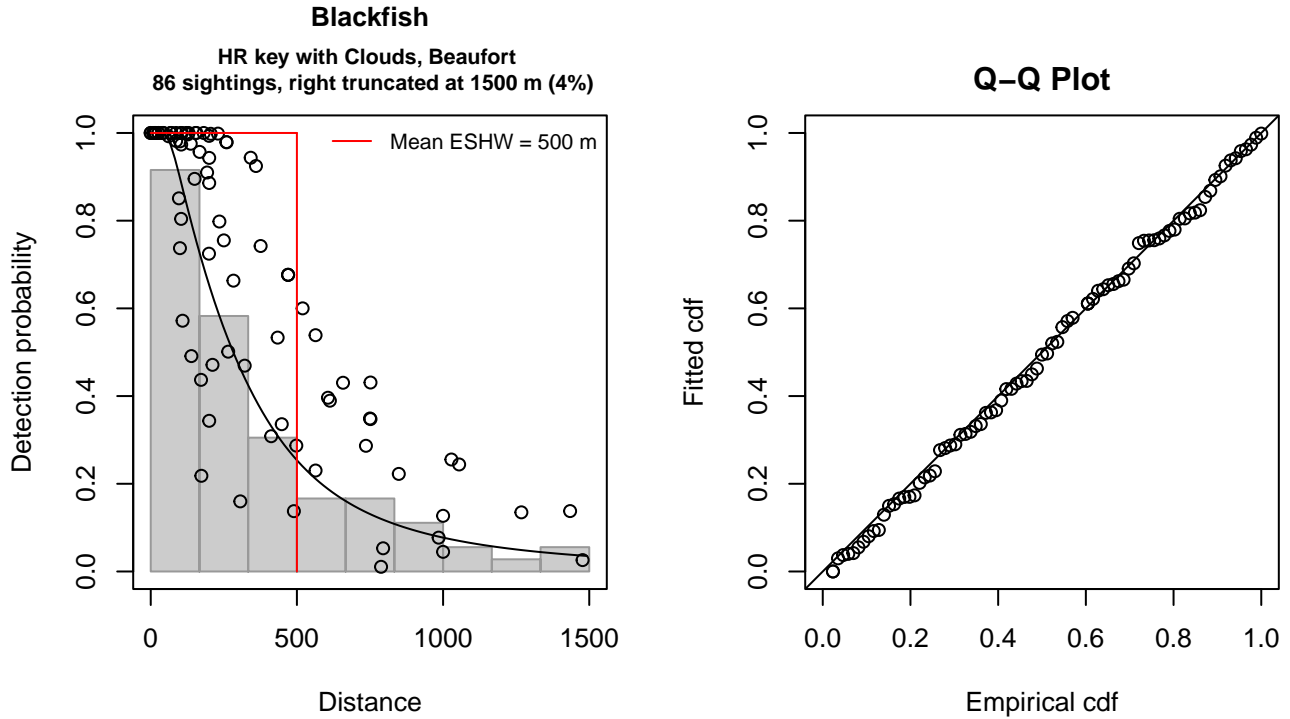| ScientificName	n
Globicephala	48
Globicephala macrorhynchus	10
Globicephala melas	3
Grampus griseus	15
Orcinus orca	6
Pseudorca crassidens	4
Total	**86**

Figure 27: Song of the Whale detection function and Q-Q plot showing its goodness of fit.

Statistical output for this detection function:

```
Summary for ds object
Number of observations :  86
Distance range         :  0  -  1500
AIC                    :  1170.598

Detection function:
 Hazard-rate key function

Detection function parameters
Scale coefficient(s):
             estimate          se
(Intercept)  6.4796997 0.26905817
Clouds      -0.1344265 0.04822789
Beaufort3-4 -0.6588095 0.31406041

Shape coefficient(s):
             estimate          se
(Intercept) 0.7265327 0.1798353
```

```
                        Estimate         SE          CV
Average p               0.265116   0.04508089  0.1700421
N in covered region  324.386340  63.44454836  0.1955833


Distance sampling Cramer-von Mises test (unweighted)
Test statistic = 0.019751  p = 0.997226
```
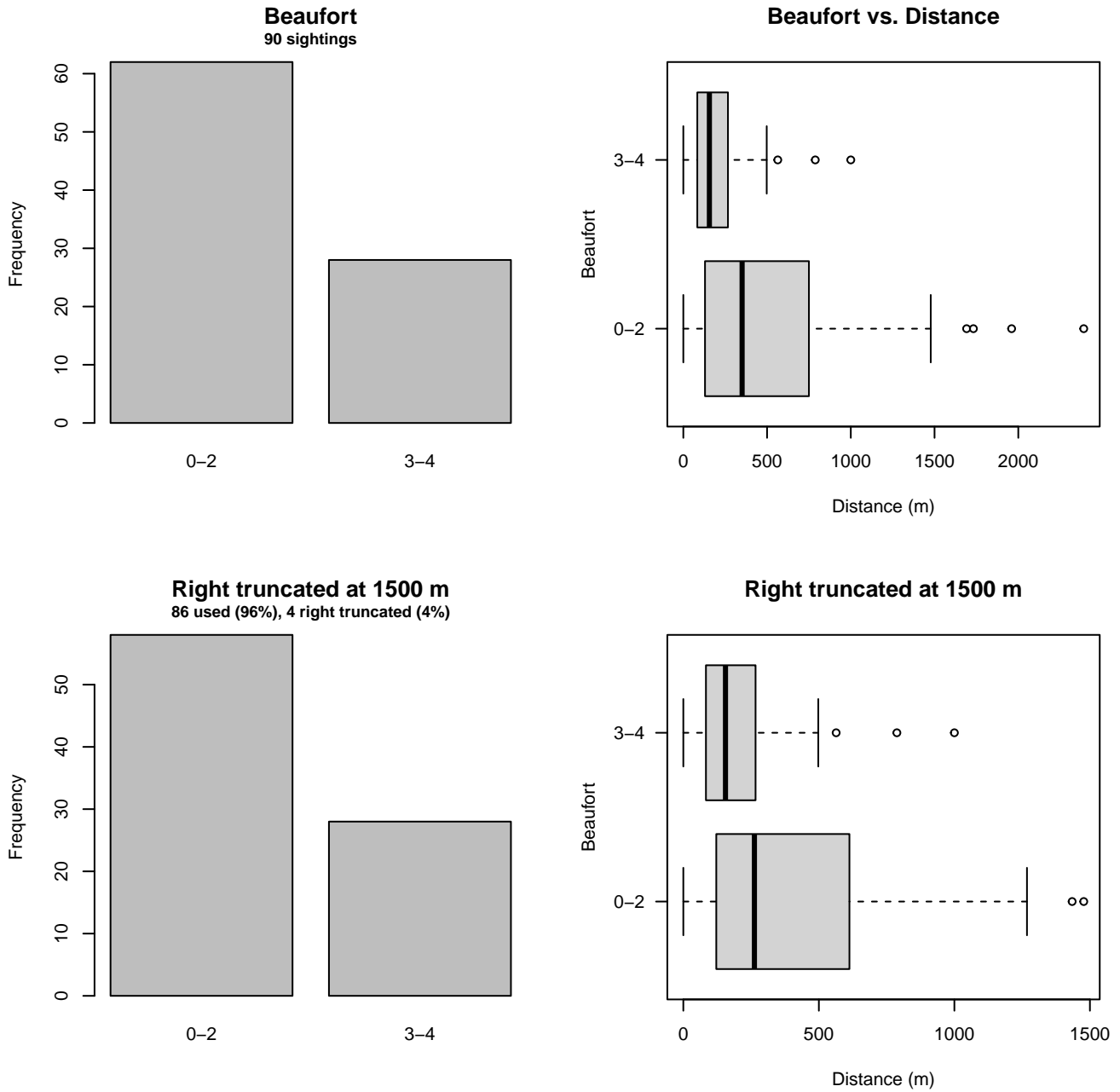

Figure 28: Distribution of the Beaufort covariate before (top row) and after (bottom row) observations were truncated to fit the Song of the Whale detection function.
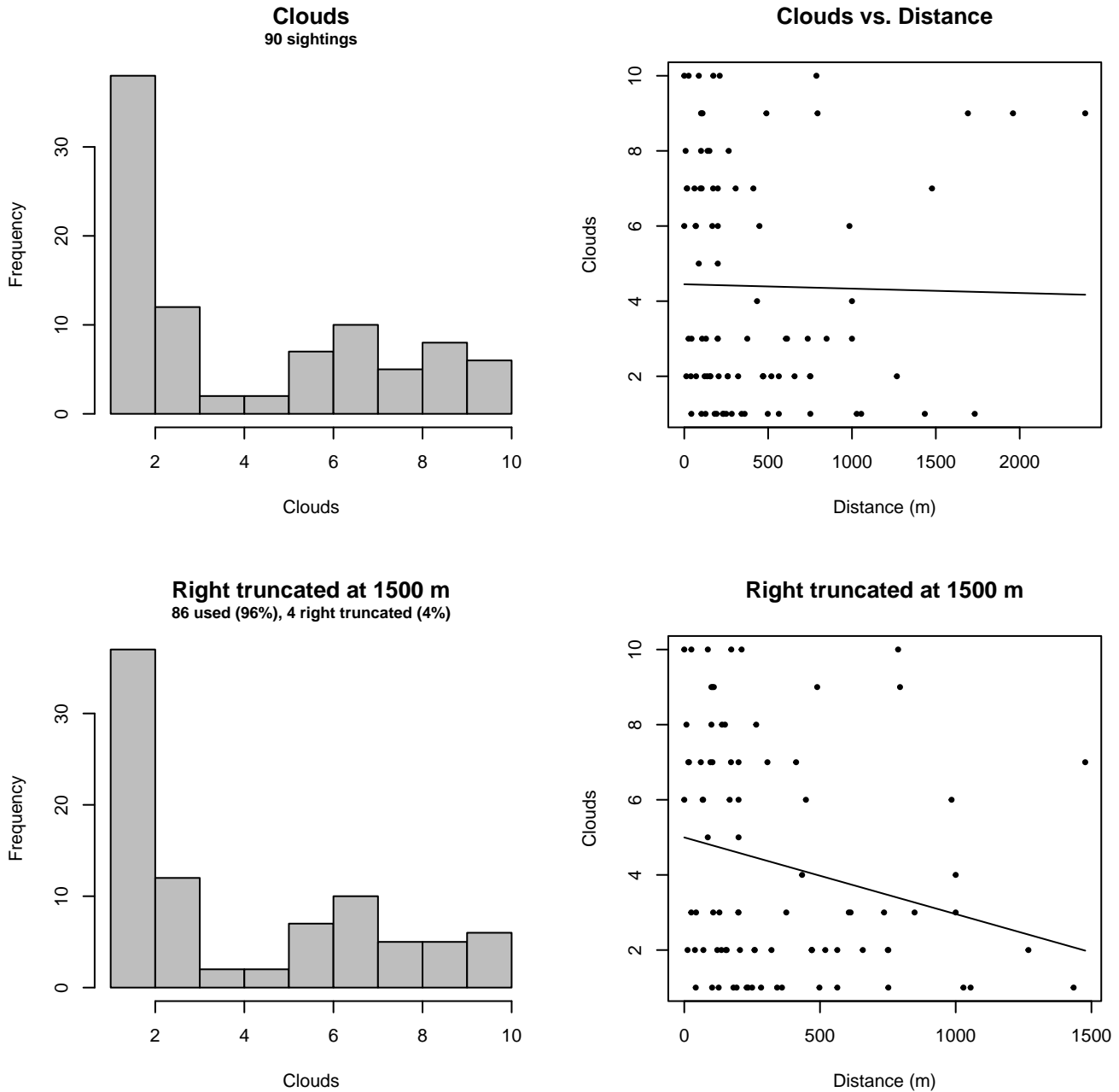
Figure 29: Distribution of the Clouds covariate before (top row) and after (bottom row) observations were truncated to fit the Song of the Whale detection function.

3 Bias Corrections

Density surface modeling methodology uses *distance sampling* (Buckland et al. 2001) to model the probability that an observer on a line transect survey will detect an animal given the perpendicular distance to it from the transect line. Distance sampling assumes that detection probability is 1 when perpendicular distance is 0. When this assumption is not met, detection probability is biased high, leading to an underestimation of density and abundance. This is known as the $g_0 < 1$ problem, where g_0 refers to the detection probability at distance 0. Modelers often try to address this problem by estimating g_0 empirically and dividing it into estimated density or abundance, thereby correcting those estimates to account for the animals that were presumed missed.

Two important sources of bias for visual surveys are known as *availability bias*, in which an animal was present on the transect line but impossible to detect, e.g. because it was under water, and *perception bias*, in which an animal was present and available but not noticed, e.g. because of its small size or cryptic coloration or behavior (Marsh and Sinclair 1989). Modelers often

estimate the influence of these two sources of bias on detection probability independently, yielding two estimates of g_0, hereafter referred to as g_{0A} and g_{0P}, and multiply them together to obtain a final, combined estimate: $g_0 = g_{0A}.g_{0P}$.

Our overall approach was to perform this correction on a per-observation basis, to have the flexibility to account for many factors such as platform type, surveyor institution, group size, group composition (e.g. singleton, mother-calf pair, or surface active group), and geographic location (e.g. feeding grounds vs. calving grounds). The level of complexity of the corrections varied by species according to the amount of information available, with North Atlantic right whale having the most elaborate corrections, derived from a substantial set of publications documenting its behavior, and various lesser known odontocetes having corrections based only on platform type (aerial or shipboard), derived from comparatively sparse information. Here we document the corrections used for killer whale.

3.1 Aerial Surveys

Reflecting the northerly distribution of the species, the only collaborating institution that reported sightings of killer whales during aerial surveys was NOAA NEFSC (Table 1). No aerial program utilized in our analysis developed a perception bias correction for killer whale. As a proxy, we used the correction for pilot whales from Palka et al. (2021), who developed perception bias corrections using two team, mark recapture distance sampling (MRDS) methodology (Burt et al. 2014) for aerial surveys conducted in 2010-2017 by NEFSC during the AMAPPS program. We applied this correction to all aerial sightings (all were from NEFSC), including from the NARWSS program (Table 15).

The NARWSS program used the same aircraft and many of the same observers as the AMAPPS program, but it flew at a higher altitude and had a searching strategy designed to maximize detections of large whales, so it is possible the AMAPPS estimate undercorrected the NARWSS data (i.e. g_{0P} for NARWSS should have been less than g_{0P} for AMAPPS). If so, it is possible this led to an underestimation of density, as 3 out of the 4 aerial sightings were reported by NARWSS.

We estimated availability bias corrections using the Laake et al. (1997) estimator, which requires mean surface and dive intervals. Although we found a number of studies that had fitted killer whales with either time-depth recorder archival tags or depth-logging satellite tags—e.g. Baird et al. (2005), Miller et al. (2010), and Reisinger et al. (2015) —none of these directly reported the mean surface and dive intervals that we needed for the Laake estimator, so we had to adapt their results to our problem.

Miller et al. (2010) used DTags to monitor 7608 dives of 11 mammal-eating killer whales in southeast Alaska and reported a mean blow rate of 68.8 blows/hour during daytime, but did not report a mean surface interval or dive interval. They did state:

> The most common surfacing behaviour of killer whales is to surface and then dive again immediately, with one breath taken during the surfacing. Killer whales are occasionally observed to drift, or log, at the surface. We inspected this in the tag records as the duration between a surfacing and start of the subsequent dive. In our records, no interval exceeded 16 s total and 99.3% of the durations between the end of a dive and the start of a subsequent dive were <5 s. Field observations indicated a whale would breathe once during such an interval.

Following this observation, we assumed that for the purpose of detection by aerial observers, the mean surface interval was 5 s. At 68.8 blows/hour, this yielded a total surface time of 344 seconds/hour, and therefore a total dive time of 3256 seconds/hour. At 68.8 blows/hour, that yielded a mean dive interval of 47.33 s.

To estimate time in view, also needed by the Laake estimator, we used results reported by Robertson et al. (2015), rescaled linearly for each survey program according to its target altitude and speed. Finally, to address the influence of group size on availability bias, we applied the group availability estimator of McLellan et al. (2018) on a per-observation basis. Following Palka et al. (2021), who also used that method, we assumed that individuals in the group dived asynchronously. The resulting g_{0A} corrections ranged from about 0.56 to 1 (Figure 30). We caution that the assumption of asynchronous diving can lead to an underestimation of density and abundance if diving is actually synchronous; see McLellan et al. (2018) for an exploration of this effect. However, if future research finds that this species conducts synchronous dives and characterizes the degree of synchronicity, the model can be updated to account for this knowledge.

We further caution that this result was derived from 11 killer whales in Alaska, which may exhibit different dive patterns than those of the western North Atlantic. As an additional comparison, we note the findings of Baird et al. (2005), who monitored 28 fish-eating killer whales with time-depth recorders in the vicinity of Vancouver Island, B.C., Canada, and reported a mean of 10.29 dives/hour during daytime for dives $\geq$ 1 min in duration. This result is very similar to that of Miller et al. (2010), who reported that during the day, dives lasting more than 57.77 seconds occurred on average 10.7 dives/hour.

Table 15: Perception bias corrections for killer whale applied to aerial surveys.

Surveys	Group Size	g_{0P}	g_{0P} Source
NEFSC	Any	0.54	Palka et al. (2021): NEFSC: pilot whales

Table 16: Surface and dive intervals for killer whale used to estimate availability bias corrections.

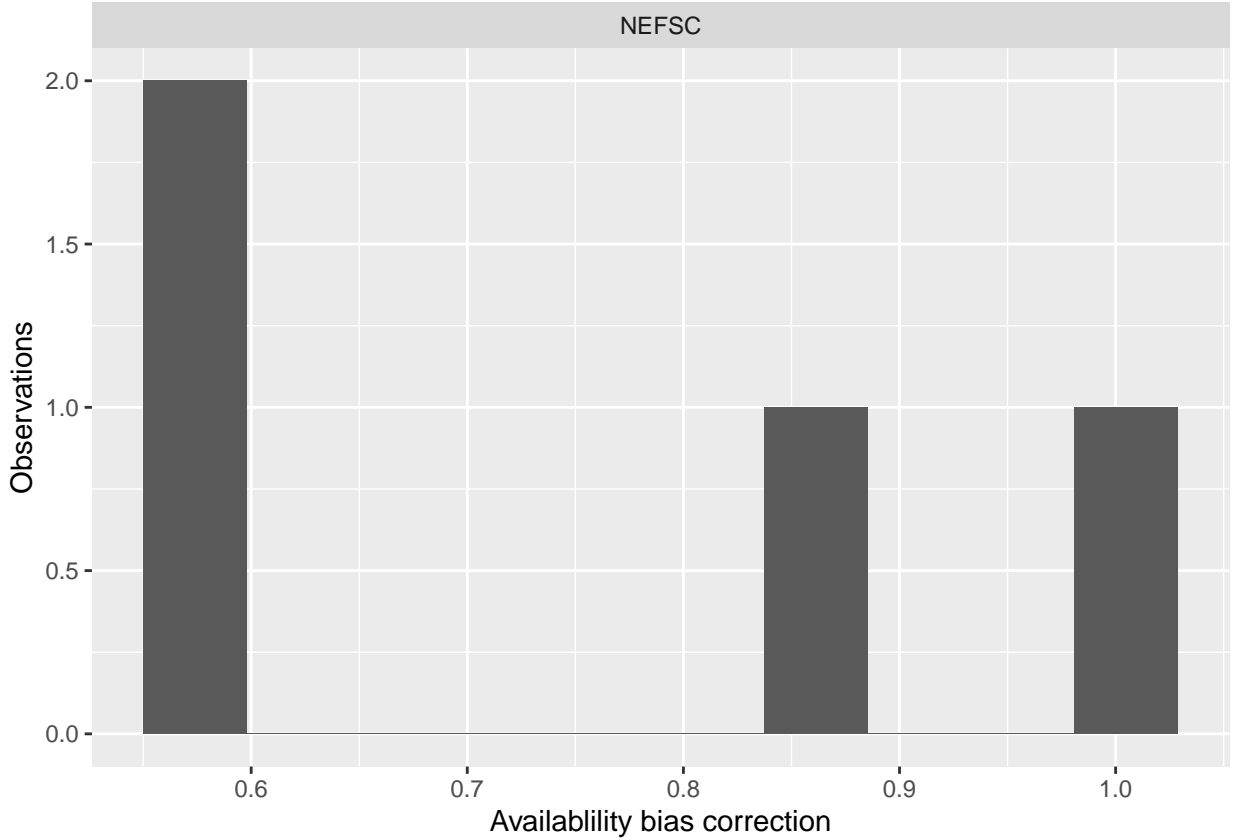| Surface Interval (s)	Dive Interval (s)	Source
5	47.3	Miller et al. (2010)

Figure 30: Availability bias corrections for killer whale for aerial surveys, by institution.

3.2   Shipboard Surveys

Most of the shipboard surveys in our analysis used high-power (25x150), pedestal-mounted binoculars. Garrison et al. (in prep.) developed perception bias corrections using two team, MRDS methodology (Burt et al. 2014) for high-power binocular surveys conducted in 2003-2018 by SEFSC during the Gulf of Mexico Marine Assessment Program for Protected Species (GoMMAPPS) and predecessor campaigns. We favored this estimate slightly over a similar effort by Palka et al. (2021) who developed estimates for the 2010-2017 AMAPPS program, because while both both estimates were made for similar guilds of "blackfish" species, the latter was more heavily dominated by Risso's dolphins and pilot whales. In any case, the estimates are similar: $g_{0P} = 0.6415$ from Garrison et al. (in prep); $g_{0P} = 0.71$ for SEFSC and $g_{0P} = 0.50$ for NEFSC from Palka et al. (2021).

We applied Garrison's estimate to all shipboard sightings. Given that the dive interval of this species (Table 16) was short relative to the amount of time a given patch of water remained in view to shipboard observers, we assumed that no availability bias correction was needed ($g_{0A} = 1$).

Table 17: Perception and availability bias corrections for killer whale applied to shipboard surveys.

Surveys	Searching Method	Group Size	g_{0P}	g_{0P} Source	g_{0A}	g_{0A} Source
All	All	≤ 20	0.6415	Garrison et al. (in prep.)	1	Assumed

4 Geographic Strata

With so few sightings, it was not possible to fit a traditional density surface model that related density observed on survey segments to environmental covariates. Nor was it possible to make proper design-based abundance estimates using traditional distance sampling (Buckland et al. 2001), because the aggregate surveys provided very heterogeneous coverage that did not together constitute a proper systematic survey design.

To provide interested parties with at least rough estimates of density in ecologically relevant geographic strata, we first split the study area into five strata (Figure 1) at major habitat boundaries. We placed our first split at the continental shelf break, defined as the 100 meter isobath, separating the study area in into shelf and offshore regions. (We manually cut across the Northeast Channel of the Gulf of Maine, so that the Gulf was considered part of the shelf.) We then split the shelf region at Cape Hatteras, a location where the Gulf Stream separates from the continental shelf, which has previously been used to delineate community structure in marine mammals (Schick et al. 2011). We also split the shelf region at the Nantucket Shoals, which separate the Gulf of Maine from the New York Bight. We split off the bays and sounds of New York, Rhode Island, and southern Massachusetts, generally at the 10 m isobath, on the basis that these inshore areas are rarely visited by cetaceans of any species. Finally, we split the offshore region at the north wall of the Gulf Stream, starting at Cape Hatteras and extending along the north wall of the Gulf Stream, as defined with a long-term climatology of total kinetic energy, to the edge of the study area.

We then derived density estimates for each stratum by fitting a model with no covariates, under the assumption that density would be distributed uniformly within the stratum. This assumption, if true, would mean we would obtain similar density estimates for a given stratum under any sampling design, and therefore it would not matter if there was some heterogeneity in sampling within the stratum. However, we strongly caution that this assumption did not hold for the other, more-common species we successfully modeled with traditional density surface modeling, as evidenced by the non-uniform patterns in density predicted by those species' models. That said, when those results are viewed at a very coarse, ecoregional scale, the boundaries used here often correlate with boundaries or strong gradients in density in those models. Thus, for the much rarer species, such as killer whale documented here, we offer this simplified approach as a rough-and-ready substitute for a full density surface model.

In this section, we present maps of each stratum that contained sightings, with tallies of effort and sightings that occurred.
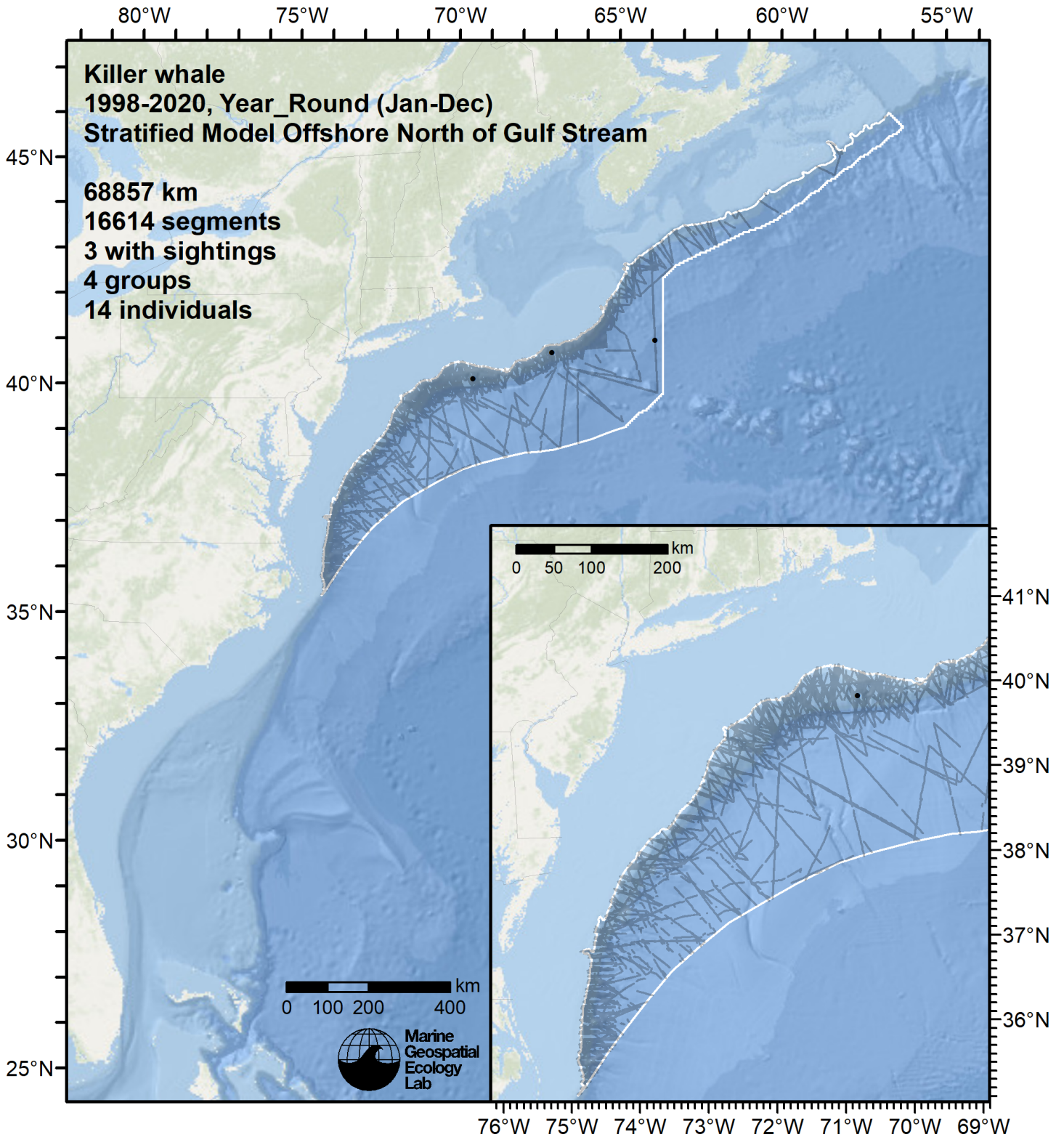
4.1 Offshore North of Gulf Stream

Figure 31: Survey segments and sightings used to estimate killer whale density for the "Offshore North of Gulf Stream" region. Black points indicate segments with observations.
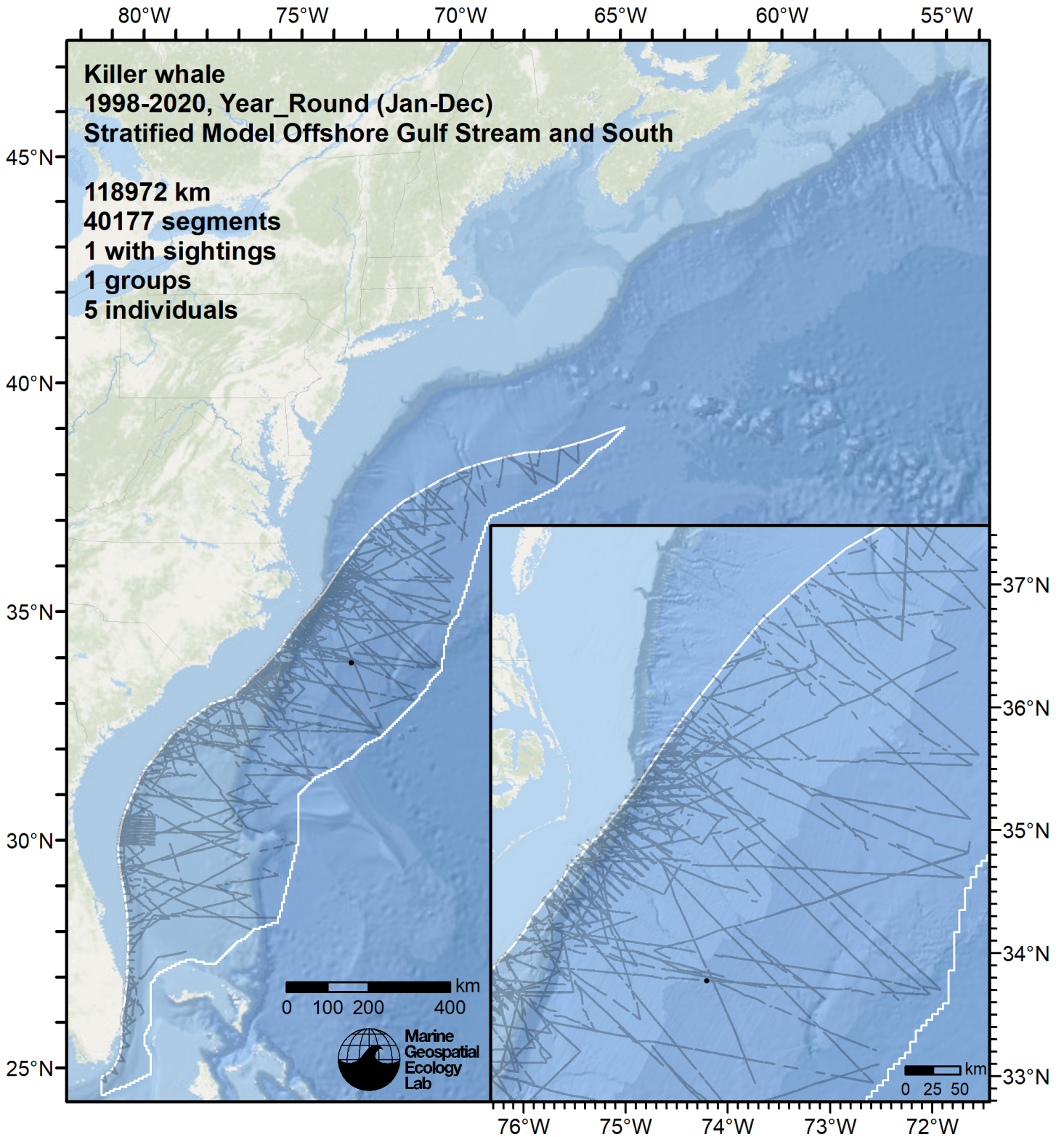
Figure 32: Survey segments and sightings used to estimate killer whale density for the "Offshore Gulf Stream and South" region. Black points indicate segments with observations.
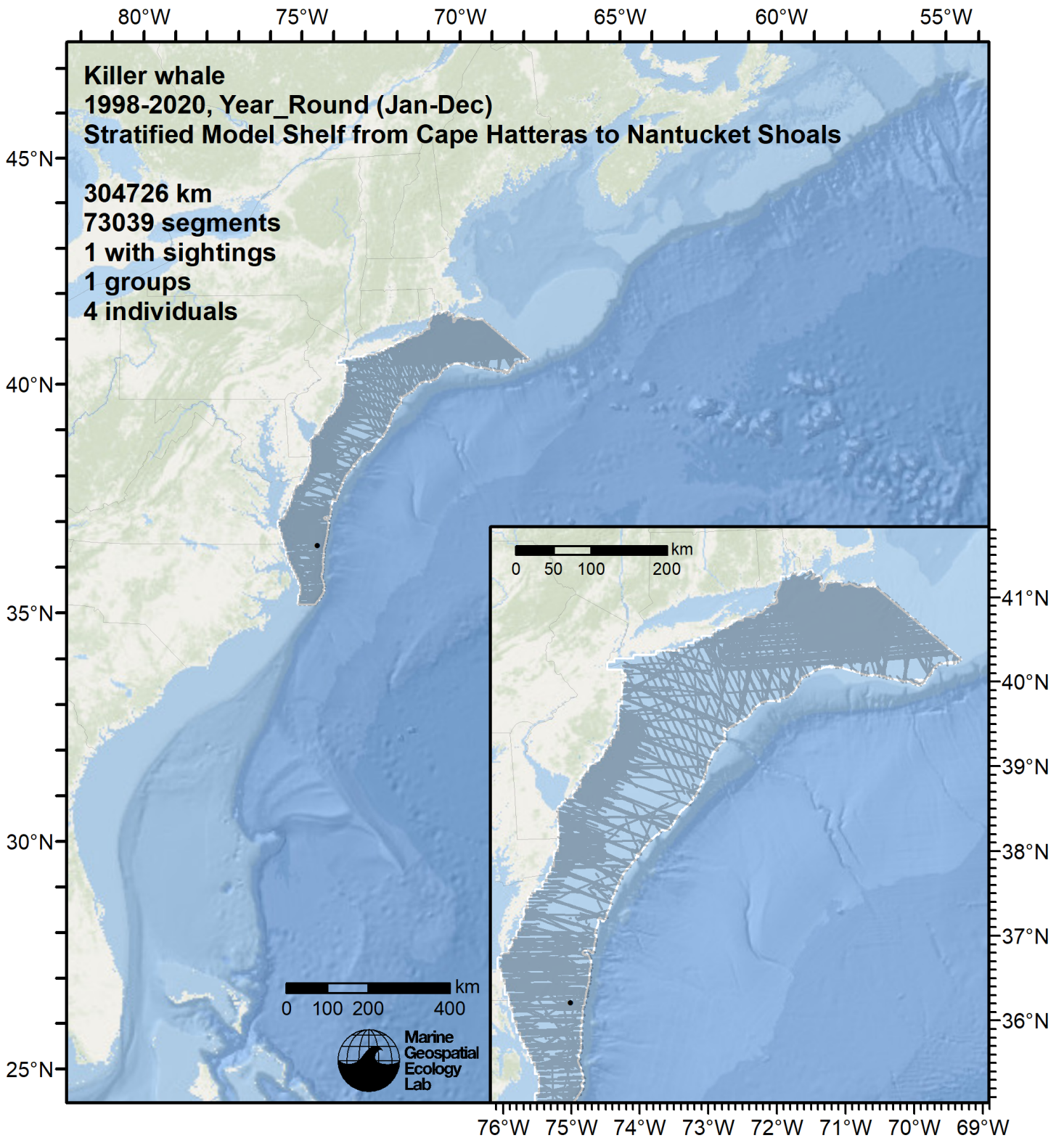
Figure 33: Survey segments and sightings used to estimate killer whale density for the "Shelf Cape Hatteras to Nantucket Shoals" region. Black points indicate segments with observations.
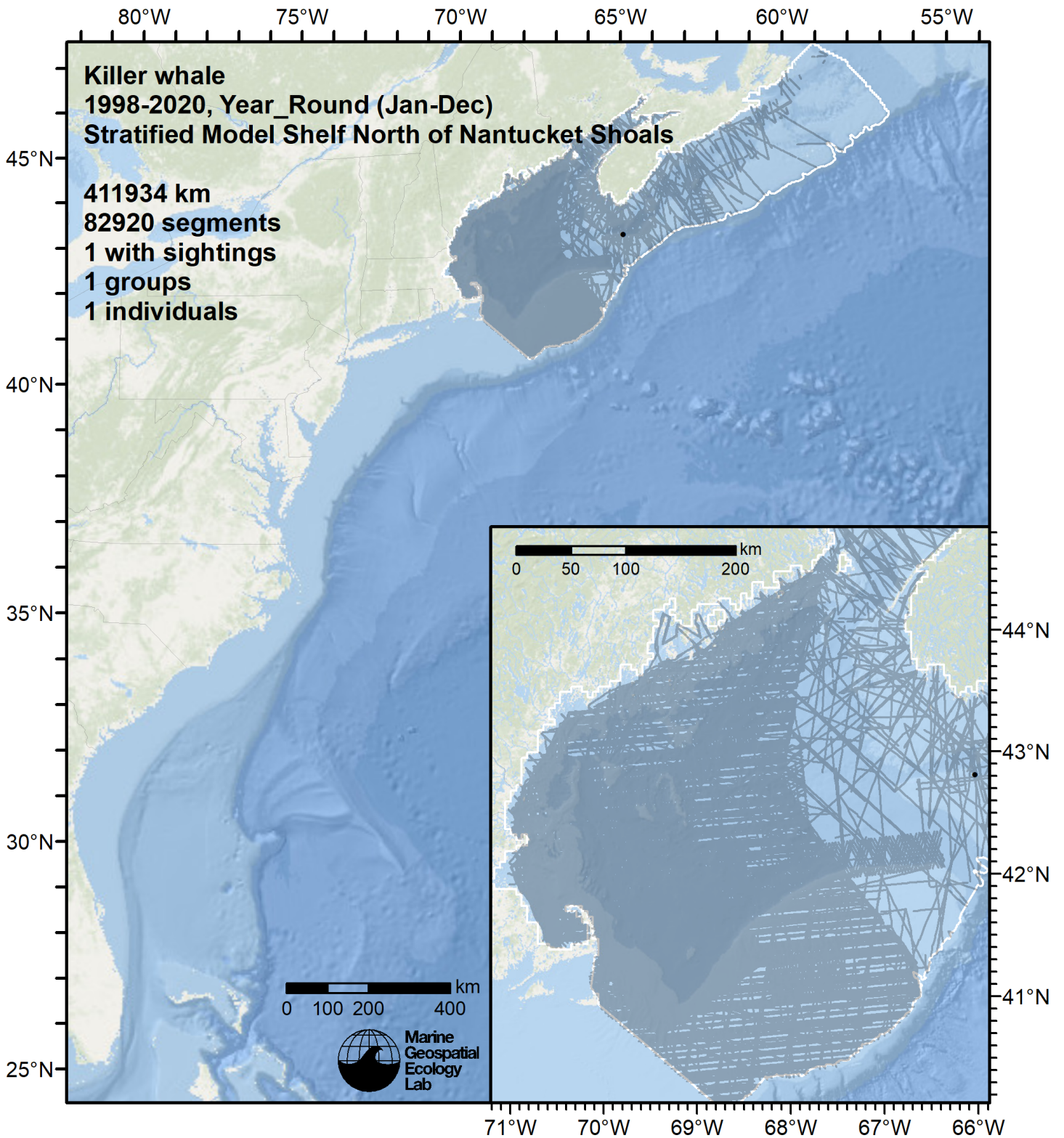
4.4 Shelf North of Nantucket Shoals

Figure 34: Survey segments and sightings used to estimate killer whale density for the "Shelf North of Nantucket Shoals" region. Black points indicate segments with observations.
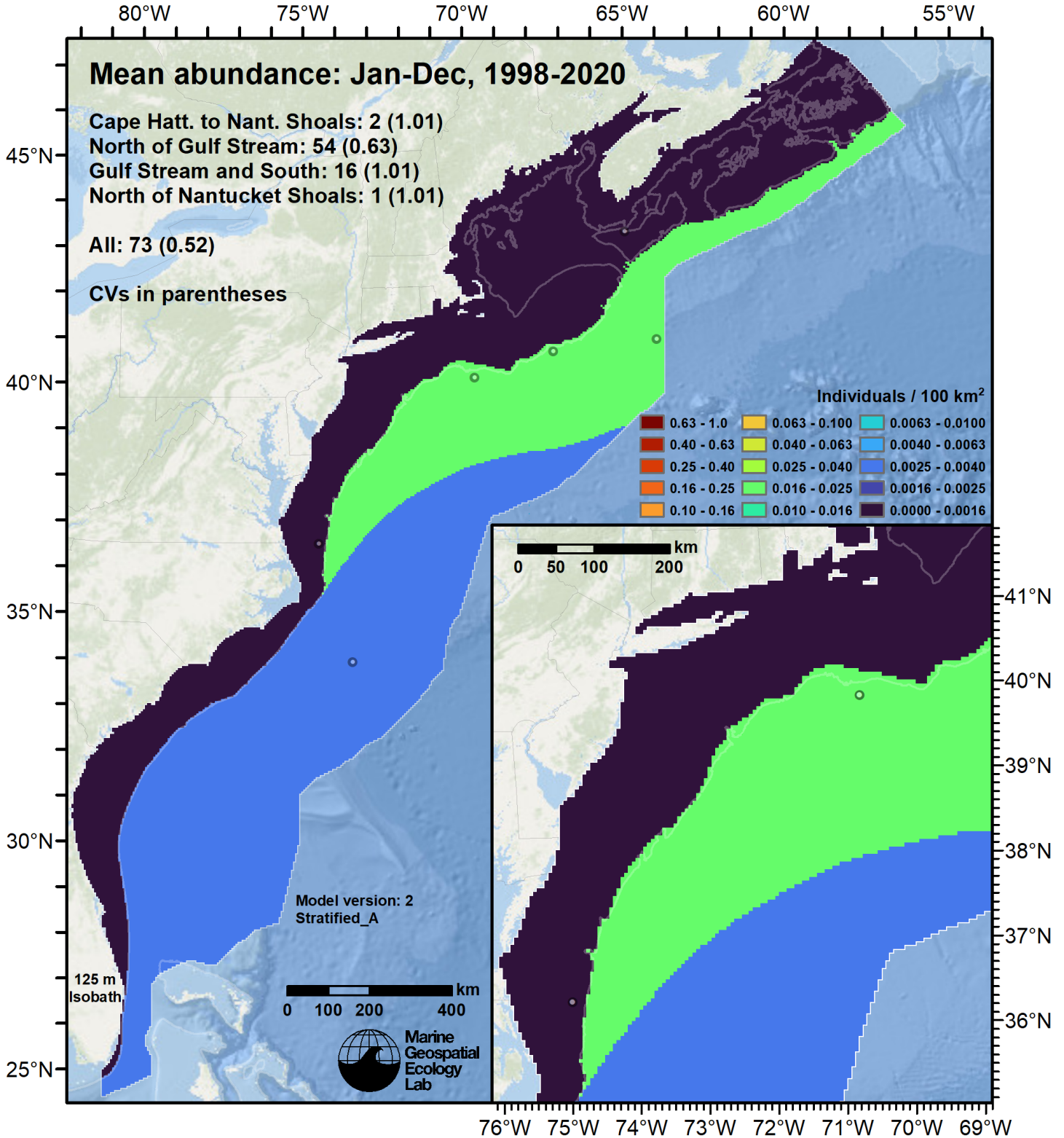
5 Predictions

5.1 Summarized Predictions

Figure 35: Killer whale density estimated for the indicated period. Open circles indicate segments with observations. The abundance estimate and its coefficient of variation (CV) are given in the subtitle.
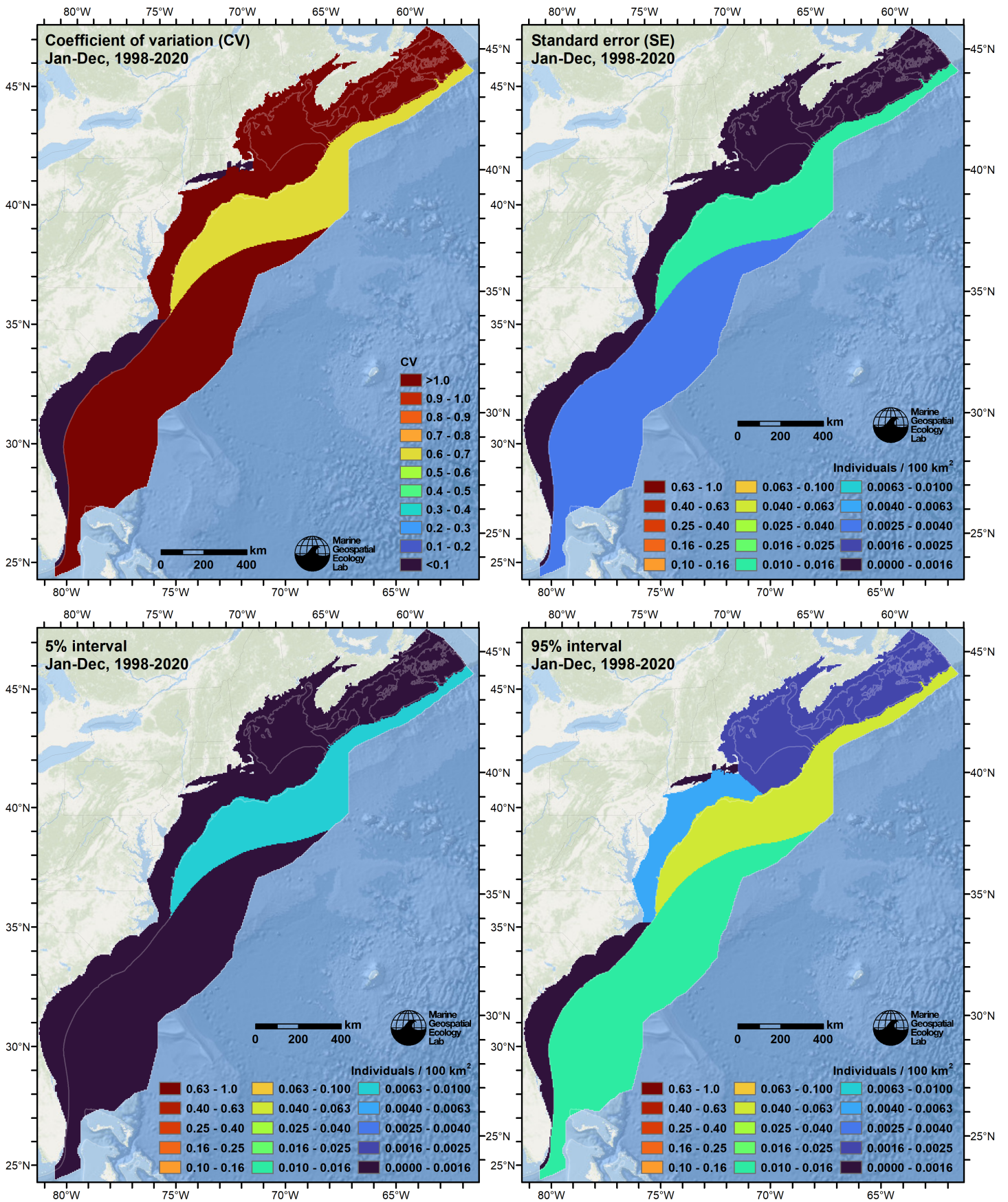
Figure 36: Uncertainty statistics for the killer whale estimated density surface (Figure 35).

Table 18: Killer whale abundance and density estimated for each stratum.

Region	Abundance	CV	95% Interval	Area (km^2)	Density (indiv. / 100 km^2)
Offshore Gulf Stream and South	16	1.008	3 - 82	499,300	0.0032
Offshore North of Gulf Stream	54	0.627	18 - 167	253,575	0.0213
Shelf Cape Hatt. to Nant. Shoals	2	1.008	0 - 8	104,425	0.0016
Shelf North of Nantucket Shoals	1	1.008	0 - 6	302,025	0.0004
Shelf South of Cape Hatteras	0	0.000	0 - 0	105,500	0.0000
Sounds of NY, RI, and MA	0	0.000	0 - 0	8,600	0.0000
Total	73	0.516	28 - 189	1,273,425	0.0057

5.2 Abundance Comparisons

5.2.1 NOAA Stock Assessment Report

The 2014 Stock Assessment Report (SAR) is the most recent to examine killer whale (Waring et al. 2015), and reports "The total number of killer whales off the eastern U.S. coast is unknown." Thus, no SAR estimate is available for comparison.
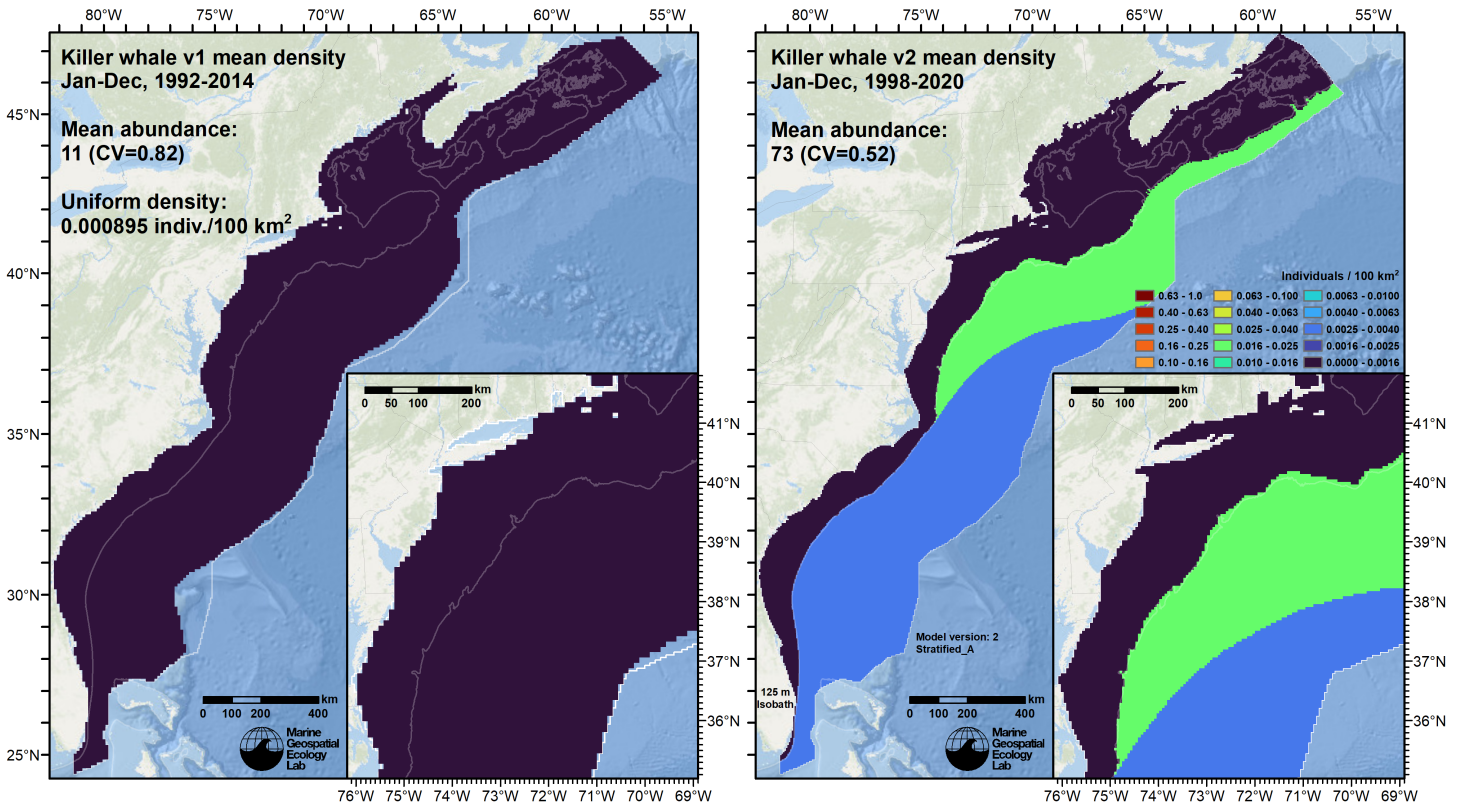
5.2.2 Previous Density Model

Figure 37: Comparison of the mean density predictions from the previous model (left) released by Roberts et al. (2016) to those from this model (right).

6 Discussion

Killer whales are widely distributed throughout the world's oceans and are found in tropical, temperate, and high-latitude waters, in both pelagic and coastal habitats (Forney and Wade 2006). They are considered rare in the Gulf of Mexico, U.S. Atlantic waters, and the Bay of Fundy, uncommon but seasonally regular in Labrador and Newfoundland, and common in the Canadian Arctic (Forney and Wade 2006). A comprehensive analysis of available systematic and opportunistic sightings

in the northwest Atlantic between 40-60 N, 40-75 °W concurred with this view (Lawson and Stevens 2014). These authors reported that almost all of the sightings in this region occurred at depths less than 200 m, but that this might reflect a bias in the distribution of observation effort, and that killer whales have been reported in mid-Atlantic waters at depths exceeding 3000 m (Lawson and Stevens 2014). For the latitudes 25-45 N, the OBIS-SEAMAP database (Halpin et al. 2009) reported sightings at depths ranging from less than 10 m to more than 5000 m; sightings were concentrated in the northern half of the region but were not absent from the southern half (http://seamap.env.duke.edu/species/180469, accessed November 15, 2022). Lawson and Stevens (2014) also reported that killer whales were sighted in their study area during all months of the year.

With insufficient sightings to model density from environmental predictors, we estimated density in five geographic strata with a simplified approach (Section 4). Total abundance was only 73 (Table 18), owing to the small number of sightings and their small group sizes. At the time of this writing, the NOAA Stock Assessment Reports had never listed an abundance estimate for killer whale in the North Atlantic. Lawson and Stevens (2014) reported a minimum number of 67 killer whales for the region 40-60 N, 40-75 °W based on photographic identification of individuals, but that this is is an underestimate of the true population. Of the 1700 photographs available, over 70% were not of sufficient quality to make an identification. They did not offer an estimate of the upper bound for the population but concluded that the northwestern Atlantic population is not as large as the northeastern Atlantic population, which may be close to 10,000 whales (Lawson and Stevens 2014). More recently, Jourdain et al. (2019) reiterated this conclusion and reported a mean abundance of 13,615 for the four North Atlantic Sighting Surveys (NASS) undertaken from 1987-2016 by cooperating countries in eastern and central North Atlantic.

In our prior model, we considered the entire study area to be a single stratum (Figure 37), on the basis that the species could, in principle, appear anywhere, given its circumglobal distribution that ranges from the tropics to the polar seas. The approach taken in the new model, to split the study area into five geographic strata based on major habitat boundaries, resulted in a similar wide spread of density, with the only the shelf south of Cape Hatteras having zero density. The absence of density there was supported by a lack of any sightings reported by OBIS-SEAMAP.

Total abundance estimated by the new model was nearly seven times higher than the prior model. This resulted both from the new model including additional sightings and from the new stratification scheme, which recognized that effort beyond the continental shelf was much lower than that over the continental shelf, resulting in much higher densities beyond the shelf.

References

Baird RW, Hanson MB, Dill LM (2005) Factors influencing the diving behaviour of fish-eating killer whales: Sex differences and diel and interannual variation in diving rates. Can J Zool 83:257–267. doi: 10.1139/z05-007

Barco SG, Burt L, DePerte A, Digiovanni R Jr. (2015) Marine Mammal and Sea Turtle Sightings in the Vicinity of the Maryland Wind Energy Area July 2013-June 2015, VAQF Scientific Report #2015-06. Virginia Aquarium & Marine Science Center Foundation, Virginia Beach, VA

Buckland ST, Anderson DR, Burnham KP, Laake JL, Borchers DL, Thomas L (2001) Introduction to Distance Sampling: Estimating Abundance of Biological Populations. Oxford University Press, Oxford, UK

Burt ML, Borchers DL, Jenkins KJ, Marques TA (2014) Using mark-recapture distance sampling methods on line transect surveys. Methods in Ecology and Evolution 5:1180–1191. doi: 10.1111/2041-210X.12294

Cole T, Gerrior P, Merrick RL (2007) Methodologies of the NOAA National Marine Fisheries Service Aerial Survey Program for Right Whales (Eubalaena glacialis) in the Northeast U.S., 1998-2006. U.S. Department of Commerce, Woods Hole, MA

Cotter MP (2019) Aerial Surveys for Protected Marine Species in the Norfolk Canyon Region: 2018–2019 Final Report. HDR, Inc., Virginia Beach, VA

Foley HJ, Paxton CGM, McAlarney RJ, Pabst DA, Read AJ (2019) Occurrence, Distribution, and Density of Protected Species in the Jacksonville, Florida, Atlantic Fleet Training and Testing (AFTT) Study Area. Duke University Marine Lab, Beaufort, NC

Forney KA, Wade PR (2006) Worldwide Distribution and Abundance of Killer Whales. In: Whales, whaling and ocean ecosystems. University of California Press, Berkeley, CA, pp 145–162

Garrison LP, Martinez A, Maze-Foley K (2010) Habitat and abundance of cetaceans in Atlantic Ocean continental slope waters off the eastern USA. Journal of Cetacean Research and Management 11:267–277.

Geo-Marine, Inc. (2010) New Jersey Department of Environmental Protection Baseline Studies Final Report Volume III: Marine Mammal and Sea Turtle Studies. Geo-Marine, Inc., Plano, TX

Halpin P, Read A, Fujioka E, Best B, Donnelly B, Hazen L, Kot C, Urian K, LaBrecque E, Dimatteo A, Cleary J, Good C, Crowder L, Hyrenbach KD (2009) OBIS-SEAMAP: The World Data Center for Marine Mammal, Sea Bird, and Sea Turtle Distributions. Oceanography 22:104–115. doi: 10.5670/oceanog.2009.42

Jourdain E, Ugarte F, Víkingsson GA, Samarra FIP, Ferguson SH, Lawson J, Vongraven D, Desportes G (2019) North Atlantic killer whale *Orcinus Orca* populations: A review of current knowledge and threats to conservation. Mam Rev 49:384–400. doi: 10.1111/mam.12168

Laake JL, Calambokidis J, Osmek SD, Rugh DJ (1997) Probability of Detecting Harbor Porpoise From Aerial Surveys: Estimating g(0). Journal of Wildlife Management 61:63–75. doi: 10.2307/3802415

Lawson JW, Stevens TS (2014) Historic and current distribution patterns, and minimum abundance of killer whales (Orcinus orca) in the north-west Atlantic. Journal of the Marine Biological Association of the United Kingdom 94:1253–1265. doi: 10.1017/S0025315413001409

Leiter S, Stone K, Thompson J, Accardo C, Wikgren B, Zani M, Cole T, Kenney R, Mayo C, Kraus S (2017) North Atlantic right whale Eubalaena glacialis occurrence in offshore wind energy areas near Massachusetts and Rhode Island, USA. Endang Species Res 34:45–59. doi: 10.3354/esr00827

Mallette SD, Lockhart GG, McAlarney RJ, Cummings EW, McLellan WA, Pabst DA, Barco SG (2014) Documenting Whale Migration off Virginia's Coast for Use in Marine Spatial Planning: Aerial and Vessel Surveys in the Proximity of the Virginia Wind Energy Area (VA WEA), VAQF Scientific Report 2014-08. Virginia Aquarium & Marine Science Center Foundation, Virginia Beach, VA

Mallette SD, Lockhart GG, McAlarney RJ, Cummings EW, McLellan WA, Pabst DA, Barco SG (2015) Documenting Whale Migration off Virginia's Coast for Use in Marine Spatial Planning: Aerial Surveys in the Proximity of the Virginia Wind Energy Area (VA WEA) Survey/Reporting Period: May 2014 - December 2014, VAQF Scientific Report 2015-02. Virginia Aquarium & Marine Science Center Foundation, Virginia Beach, VA

Mallette SD, McAlarney RJ, Lockhart GG, Cummings EW, Pabst DA, McLellan WA, Barco SG (2017) Aerial Survey Baseline Monitoring in the Continental Shelf Region of the VACAPES OPAREA: 2016 Annual Progress Report. Virginia Aquarium & Marine Science Center Foundation, Virginia Beach, VA

Marsh H, Sinclair DF (1989) Correcting for Visibility Bias in Strip Transect Aerial Surveys of Aquatic Fauna. The Journal of Wildlife Management 53:1017. doi: 10.2307/3809604

McAlarney R, Cummings E, McLellan W, Pabst A (2018) Aerial Surveys for Protected Marine Species in the Norfolk Canyon Region: 2017 Annual Progress Report. University of North Carolina Wilmington, Wilmington, NC

McLellan WA, McAlarney RJ, Cummings EW, Read AJ, Paxton CGM, Bell JT, Pabst DA (2018) Distribution and abundance of beaked whales (Family Ziphiidae) Off Cape Hatteras, North Carolina, U.S.A. Marine Mammal Science. doi: 10.1111/mms.12500

Miller PJO, Shapiro AD, Deecke VB (2010) The diving behaviour of mammal-eating killer whales (*Orcinus Orca*): Variations with ecological not physiological factors. Canadian Journal of Zoology 88:1103–1112. doi: 10.1139/Z10-080

Mullin KD, Fulling GL (2003) Abundance of cetaceans in the southern U.S. North Atlantic Ocean during summer 1998. Fishery Bulletin 101:603–613.

O'Brien O, Pendleton DE, Ganley LC, McKenna KR, Kenney RD, Quintana-Rizzo E, Mayo CA, Kraus SD, Redfern JV (2022) Repatriation of a historical North Atlantic right whale habitat during an era of rapid climate change. Sci Rep 12:12407. doi: 10.1038/s41598-022-16200-8

Palka D, Aichinger Dias L, Broughton E, Chavez-Rosales S, Cholewiak D, Davis G, DeAngelis A, Garrison L, Haas H, Hatch J, Hyde K, Jech M, Josephson E, Mueller-Brennan L, Orphanides C, Pegg N, Sasso C, Sigourney D, Soldevilla M, Walsh H (2021) Atlantic Marine Assessment Program for Protected Species: FY15 – FY19 (OCS Study BOEM 2021-051). U.S. Deptartment of the Interior, Bureau of Ocean Energy Management, Washington, DC

Palka DL (2006) Summer abundance estimates of cetaceans in US North Atlantic navy operating areas (NEFSC Reference Document 06-03). U.S. Department of Commerce, Northeast Fisheries Science Center, Woods Hole, MA

Palka DL, Chavez-Rosales S, Josephson E, Cholewiak D, Haas HL, Garrison L, Jones M, Sigourney D, Waring G, Jech M, Broughton E, Soldevilla M, Davis G, DeAngelis A, Sasso CR, Winton MV, Smolowitz RJ, Fay G, LaBrecque E, Leiness JB, Dettloff K, Warden M, Murray K, Orphanides C (2017) Atlantic Marine Assessment Program for Protected Species: 2010-2014 (OCS Study BOEM 2017-071). U.S. Deptartment of the Interior, Bureau of Ocean Energy Management, Washington, DC

Quintana-Rizzo E, Leiter S, Cole T, Hagbloom M, Knowlton A, Nagelkirk P, O'Brien O, Khan C, Henry A, Duley P, Crowe L, Mayo C, Kraus S (2021) Residency, demographics, and movement patterns of North Atlantic right whales Eubalaena

glacialis in an offshore wind energy development area in southern New England, USA. Endang Species Res 45:251–268. doi: 10.3354/esr01137

Read AJ, Barco S, Bell J, Borchers DL, Burt ML, Cummings EW, Dunn J, Fougeres EM, Hazen L, Hodge LEW, Laura A-M, McAlarney RJ, Peter N, Pabst DA, Paxton CGM, Schneider SZ, Urian KW, Waples DM, McLellan WA (2014) Occurrence, distribution and abundance of cetaceans in Onslow Bay, North Carolina, USA. Journal of Cetacean Research and Management 14:23–35.

Redfern JV, Kryc KA, Weiss L, Hodge BC, O'Brien O, Kraus SD, Quintana-Rizzo E, Auster PJ (2021) Opening a Marine Monument to Commercial Fishing Compromises Species Protections. Front Mar Sci 8:645314. doi: 10.3389/fmars.2021.645314

Reisinger RR, Keith M, Andrews RD, de Bruyn PJN (2015) Movement and diving of killer whales (Orcinus orca) at a Southern Ocean archipelago. Journal of Experimental Marine Biology and Ecology 473:90–102. doi: 10.1016/j.jembe.2015.08.008

Roberts JJ, Best BD, Mannocci L, Fujioka E, Halpin PN, Palka DL, Garrison LP, Mullin KD, Cole TVN, Khan CB, McLellan WA, Pabst DA, Lockhart GG (2016) Habitat-based cetacean density models for the U.S. Atlantic and Gulf of Mexico. Scientific Reports 6:22615. doi: 10.1038/srep22615

Roberts JJ, Yack TM, Halpin PN (2023) Marine mammal density models for the U.S. Navy Atlantic Fleet Training and Testing (AFTT) study area for the Phase IV Navy Marine Species Density Database (NMSDD), Document Version 1.3. Duke University Marine Geospatial Ecology Lab, Durham, NC

Robertson FC, Koski WR, Brandon JR, Thomas TA, Trites AW (2015) Correction factors account for the availability of bowhead whales exposed to seismic operations in the Beaufort Sea. Journal of Cetacean Research and Management 15:35–44.

Ryan C, Boisseau O, Cucknell A, Romagosa M, Moscrop A, McLanaghan R (2013) Final report for trans-Atlantic research passages between the UK and USA via the Azores and Iceland, conducted from R/V Song of the Whale 26 March to 28 September 2012. Marine Conservation Research International, Essex, UK

Schick R, Halpin P, Read A, Urban D, Best B, Good C, Roberts J, LaBrecque E, Dunn C, Garrison L, Hyrenbach K, McLellan W, Pabst D, Palka D, Stevick P (2011) Community structure in pelagic marine mammals at large spatial scales. Marine Ecology Progress Series 434:165–181. doi: 10.3354/meps09183

Stone KM, Leiter SM, Kenney RD, Wikgren BC, Thompson JL, Taylor JKD, Kraus SD (2017) Distribution and abundance of cetaceans in a wind energy development area offshore of Massachusetts and Rhode Island. J Coast Conserv 21:527–543. doi: 10.1007/s11852-017-0526-4

Waring GT, Josephson E, Maze-Foley K, Rosel PE, Byrd B, Cole TVN, Engleby L, Garrison LP, Hatch J, Henry A, Horstman SC, Litz J, Mullin KD, Orphanides C, Pace RM, Palka DL, Lyssikatos MC, Wenzel FW (2015) US Atlantic and Gulf of Mexico Marine Mammal Stock Assessments - 2014. NOAA National Marine Fisheries Service, Northeast Fisheries Science Center, Woods Hole, MA

Whitt AD, Powell JA, Richardson AG, Bosyk JR (2015) Abundance and distribution of marine mammals in nearshore waters off New Jersey, USA. Journal of Cetacean Research and Management 15:45–59.